Quantitative Systems Toxicology (DILIsym®) Modeling of the Acetaminophen Mode of Action (MOA) Pathway Supports that It Is Not a Carcinogenic Hazard

Supplementary Information Supporting the Main Submission to the California Carcinogen Identification Committee

Submitted by the:

Consumer Healthcare Products Association

November 4, 2019

1   Executive Summary

The objective of this document is to present the modeling and simulations results that were obtained using the DILIsym® Quantitative Systems Toxicology (QST) platform in support of a broader assessment of the carcinogenicity hazard potential of acetaminophen. The DILIsym QST platform was developed to evaluate and understand potential mechanisms of drug-induced liver injury and has been validated using experimental data for compounds such as acetaminophen.

This document serves as **a companion document** to a comprehensive weight of evidence assessment of the animal carcinogenicity, genetic toxicology and epidemiology data for acetaminophen that is being submitted in response to the OEHHA Hazard Identification Document (HID). It should be viewed as a supporting document and not read in isolation.

QST modeling provides a physiologically-based mathematical approach to simulate the potential impact of variation in underlying biological parameters across a patient population on toxicity, and to extrapolate/interpolate exposures and margins where they may not have been directly measured experimentally.

In the context of this carcinogenicity hazard assessment of acetaminophen, the DILIsym platform was used to

- Simulate different acetaminophen dosing schemes (therapeutic, supratherapeutic, and overdose conditions) in 300 unique simulated human individuals and animal cohorts (mirroring the cohorts in the carcinogenicity studies) and evaluate the impact of potential variability in their underlying biochemical and cellular pathways. A database of the simulation results was compiled allowing visualization of the dose response and kinetics changes in parameters such as glutathione, protein adducts, mitochondrial inhibition, and cell death.
- Assess the potential impact of population variability in baseline GSH levels, drug metabolism, pharmacokinetics, and antioxidant clearance capacity and the implications for its carcinogenicity potential in patient populations.
- Estimate the exposures to acetaminophen and its metabolites in the animal carcinogenicity studies, where the exposures were not measured, and compare them to exposures in humans at therapeutic and supratherapeutic chronic exposures and also following acute overdose
- Simulate conditions of overdose hepatotoxicity and evaluate the implications for acetaminophen becoming a hazard for carcinogenicity

Taken together, the modeling and simulations results, consistent with extensive mechanistic experimental data, support that at therapeutic exposures, cellular glutathione deactivates the NAPQI metabolite and there is sufficient buffering capacity to prevent any meaningful protein adduct formation or oxidative stress. As exposures increase to overdose conditions, cell death occurs before any adverse conditions occur (e.g. oxidative stress or DNA damage) that could result in carcinogenicity. Simulations on the exposures in the animal carcinogenicity studies and in humans support that the animal carcinogenicity studies adequately evaluated the range of exposure conditions in humans. The modeling and simulation results also support that acetaminophen is not a carcinogenicity hazard to human health under any conditions, including at therapeutic and supratherapeutic doses and an acute overdose.

Table of Contents

2   Introduction and Background

Acetaminophen has a long history of safe use in humans at therapeutic doses but causes liver injury in animals and humans at very high doses. As part of a broader science and weight-of-evidence assessment of the carcinogenicity hazard potential of acetaminophen, we utilized a well-established Quantitative Systems Toxicology (QST) platform (DILIsym) to address key aspects of this question. The model was developed and validated using experimental and clinical data on acetaminophen pharmacokinetics, metabolism, disposition and hepatotoxicity, and on overdose. It can be used to evaluate the effect of drug exposure and metabolism on cell death via a mathematical construct composed of ordinary differential equations. The unifying theme of this analysis was a focus on the mode of action pathway by which acetaminophen causes liver toxicity at high doses (i.e. overdose).

The initial development of DILIsym was directly encouraged and financially supported by the United States Food and Drug Administration (FDA) through a Cooperative Research and Development Agreement, or CRADA ("*Development of Drug-Induced Liver Injury (DILI) PhysioLab Platform*" sponsored by Dr. Mark Avigan and Dr. John Senior). The various groups involved in the development of the platform, including FDA, agreed from the outset that acetaminophen was a prototypical compound due to its history of causing drug-induced liver injury in people under overdose conditions. Thus, DILIsym was initially focused on simulating the events associated with acetaminophen liver toxicity. Most importantly, DILIsym has been used to address key questions associated with acetaminophen toxicity, and these results have been published (1–3). An overview of the model and the experimental data that were used to develop the model are described below.

3   General Overview of Mechanisms of Drug Induced Liver Injury (DILI) in DILIsym Software

The DILIsym software platform has been developed by DILIsym Services Inc., a Simulations Plus Company, over the last 10 years for the process of predicting and understanding drug-induced liver injury (DILI) in humans and animals (rats, mice, dogs). The QST platform has been heavily peer reviewed, both in terms of the methods and data associated with its development, and applications or case studies of software use (1–23). DILIsym includes three primary mechanisms that can combine with the characteristics of a given compound and/or metabolite to cause DILI. Bile acid toxicity, mitochondrial toxicity, and oxidative stress are the three mechanisms included in DILIsym, and they can combine in multiple ways to disrupt normal hepatocellular function and elicit hepatocellular apoptosis and/or necrosis. A summary diagram of DILIsym version 8A is below in Figure 1.

Figure 1– Summary Diagram of DILIsym Software Version 8A
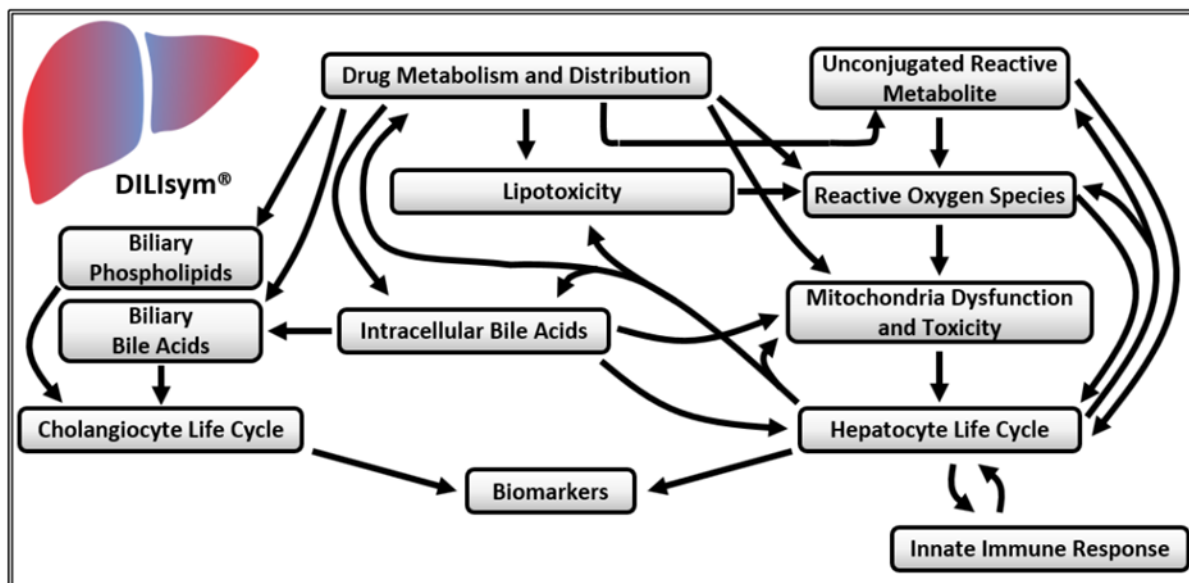
The DILIsym software represents bile acid enterohepatic circulation via bile acid transporters. More specifically, hepatocyte uptake of bile acids from blood occurs by NTCP-mediated transport. Bile acid efflux occurs via BSEP canalicular transport and multidrug resistance-associated proteins 3 and 4 (MRP3 and MRP4) basolateral transport. Drug-mediated inhibition of BSEP, MRP3, and/or MRP4 would be expected to result in hepatocellular bile acid accumulation, culminating in bile acid-mediated toxicity, while drug-mediated inhibition of NTCP could mitigate this effect. Drug-mediated inhibition of transporters can be assessed in laboratory experiments using isolated hepatocytes or membrane vesicles expressing the transporter of interest. Importantly, the hepatotoxic potential of transporter inhibition can be influenced by type of inhibition (*e.g.,* competitive *vs.* non-competitive) as well as potency of inhibition (6). This can influence the selected *in vitro* experiments, as inhibition type can be determined from experimental K_i, but not IC_{50}, data.

DILIsym represents mitochondrial bioenergetics leading to adenosine triphosphate (ATP) production in hepatocytes. Mitochondrial function in other liver cell populations *(e.g.,* Kupffer cells) is not represented. Compounds may induce mitochondrial dysfunction by inhibiting the electron transport chain (ETC), by inhibiting the mitochondrial F_1F_O ATPase, or by uncoupling mitochondrial respiration from mitochondrial ATP synthesis. Compound effects on hepatocyte mitochondrial function can be assessed in laboratory experiments by measuring hepatocyte respiration following culture with compound in a Seahorse XF Analyzer (Agilent Technologies, CA).

DILIsym represents the generation of oxidative stress or reactive oxygen species (ROS) in response to compound exposure. ROS accumulation can ultimately reduce mitochondrial ATP synthesis, leading to hepatocyte death, as well as directly lead to caspase activation and apoptosis. There are several experimental methods that can be used to measure compound-induced oxidative stress, including assays for lipid peroxidation, *e.g.,* thiobarbituric acid reactive substances (TBARS) assay, indirect measurement of superoxide, *e.g.,* dihydroethidium (DHE) fluorescence assay, and indirect measures of multiple ROS,

e.g., 2',7' –dichlorofluorescin diacetate (DCFDA) fluorescence assay; hydroxyphenyl fluorescein (HPF) fluorescence assay.

DILIsym represents the generation of reactive metabolites from parent compounds or stable metabolites. Once generated, the reactive metabolite within DILIsym can 1) be cleared by irreversible conjugation with GSH, 2) be cleared through binding to other proteins within the hepatocyte (a general protein adduction pathway not specific to any particular proteins), or be deactivated through a generic deactivation pathway which would represent an alternative clearance mechanism. Within this framework, excessive generation of the reactive metabolite can lead to depletion of GSH in the liver. Once GSH is depleted, the free reactive metabolite concentration increases. If the reactive metabolite is assumed to cause ROS (and parameterized as such in DILIsym), such as has been assumed for the reactive metabolite of acetaminophen, the increase in free concentration leads to excess ROS that reduces ATP as described in the preceding paragraph (1,2,24).

Toxicity in hepatocytes could be driven by drug concentrations at different biophases (e.g., total concentration, unbound cytosolic concentration, mitochondrial concentration) depending on participating mechanisms, but currently there is no consensus on which biophase concentration drives each mechanism. In DILIsym, bile acid transporter inhibition, mitochondrial dysfunction, and ROS generation are based on the total intracellular concentration of the drug and its metabolites in the liver. For mitochondrial dysfunction and ROS generation mechanisms which are assessed in whole cell-based assay systems, intracellular drug binding does not affect toxicity parameters and DILIsym predictions because total intracellular drug concentrations experimentally measured in *in vitro* assays are used to calculate DILIsym toxicity parameters. Assuming intracellular binding and distribution of drugs in *in vitro* cells resemble those quantities *in vivo*, parameters that define quantitative relationships between total intracellular drug concentrations and toxicity outcomes *in vitro* can be used for *in vivo* predictions.

For bile acid transporter inhibition which is measured in isolated systems such as membrane vesicles, one might postulate that unbound cytosolic drug concentrations represent a better biophase to be employed for prediction of *in vivo* hepatotoxicity. However, it is the experience of the DILIsym team that using total concentration (protein bound and unbound) leads to more accurate predictions than using free concentrations for over 40 bile acid transporter inhibitors tested in DILIsym. There exist several possible explanations as to why the use of total drug concentrations outperforms the use of unbound concentrations. First, although vesicular transporter inhibition assay systems do not contain proteins, drugs may bind to vesicles and lipid membranes, which are not considered when estimating inhibition constants. Also, bile acids themselves are known to be highly bound to intracellular proteins and lipids. Thus, intracellular binding of both bile acids and drugs need to be considered when making predictions, but our current understanding about the complex drug-bile acid-transporter interaction in the intracellular environment is limited.

While the DILIsym team continues to investigate these complex interactions to improve the mechanistic representation of bile acid transporter inhibition within DILIsym and *in vitro* to *in vivo* translation of transporter inhibition constants, the current version of DILIsym employs the total intracellular drug concentrations, which have accurately predicted clinical hepatotoxicity of over 40 exemplar compounds tested in DILIsym that exhibit transporter inhibition.

DILIsym represents synthesis and clearance of bilirubin via bilirubin enzymes and transporters. More specifically, OATP1B1/1B3 facilitates hepatic uptake of unconjugated bilirubin and hepatic reuptake of

conjugated bilirubin; UGT1A1 mediates the conversion of unconjugated bilirubin, and MRP2 and MRP3 transport conjugated bilirubin into the bile and sinusoidal blood, respectively (23). Each of the enzyme- or transporter-mediated processes can be competitively inhibited by drugs or metabolites which may result in hyperbilirubinemia, even in the absence of overt liver injury.

4   Validation of the DILIsym Acetaminophen Simulations

The DILIsym acetaminophen model validation data sets are contained in peer reviewed publications and their large supplemental data sets, including extensive comparisons of the simulation results to experimental data in the following areas (1–3):

1. Acetaminophen ADME and pharmacokinetics in humans, mice, and rats across a wide range of doses covering therapeutic, supratherapeutic, and overdose scenarios;
2. Kinetic and dose response information for GSH depletion, ROS generation, mitochondrial dysfunction (ATP production and concentration decreases) and protein adduct formation across doses in mice and rats;
3. Kinetic and dose response information for liver ATP depletion, hepatocyte death and regeneration, and associated clinical biomarkers (e.g. aminotransferases, bilirubin) across doses in humans, rats, and mice.

A summary of the experimental parameters that have been used to develop and validate the DILIsym simulations along with links to the corresponding figures in this document provided in Table 1.

Table 1- Summary of the experimental parameters that have been used to develop and validate the DILIsym simulations.

Parameter / Endpoint	Experimental Data Supporting Kinetics	Experimental Data Supporting Dose Response	Model Comparison to Experimental Data
Acetaminophen and Metabolite ADME and Pharmacokinetics	✓	✓	Figs 2, 3, 8, 9 Refs (1–3)
Glutathione Depletion	✓	✓	Figs 10, 11, 13, 14, 20, 23 Refs (1–3)
Hepatoxicity	✓	✓	Figs 4, 5, 6, 7, 17, 18; Table 2 Refs (1–3)
Oxidative Stress/ Reactive Oxygen Species Generation	✓	✓	Refs (1–3)
Mitochondrial Inhibition/Dysfunction	✓	✓	Figs 15, 16 Refs (1–3)
Protein Adduct Formation	✓	✓	Figs 12, 13, 14, 20, 23 Refs (1–3)

The human acetaminophen model in DILIsym was constructed and validated using both clinical and preclinical data. The model represents the three metabolic pathways of acetaminophen as well as the GSH conjugation and protein adduct formation of the reactive metabolite, NAPQI. The production and clearance of acetaminophen-mediated reactive oxygen species (ROS) and associated mitochondrial dysfunction (ATP production inhibition) effects are also calibrated and validated in the model. The ROS and ATP inhibition mechanisms are in turn linked to processes that determine the fate (necrosis,

apoptosis) of hepatocytes and a cascade of downstream effects including immune responses. The acetaminophen model was established as an integral part of the DILIsym software and, as noted above, has been extensively peer reviewed (1–3).

4.1 Human validation of the physiologically-based pharmacokinetic model of acetaminophen and metabolites

Highlights of pharmacokinetic, mechanistic, and clinical biomarker experimental data that were used to validate the DILIsym physiologically-based pharmacokinetic model of acetaminophen and metabolites (PBPK)are provided in the sections that follow. For the full spectrum of this validation, please see the acetaminophen related references (1–3), with special emphasis on their supplements. The most critical validation of the human DILIsym PBPK model for acetaminophen is urinary excretion data for the three primary metabolic pathways (25) compared to simulation results, as shown below in Figure 2.

Figure 2 - Selected pharmacokinetic data used to optimize the acetaminophen metabolism sub-model for humans, shown with the corresponding simulation results produced with the DILIsym model. (A) Measured cumulative acetaminophen-sulfate conjugates excreted in urine over 24 hours (▲), simulated cumulative acetaminophen-sulfate conjugates excreted in urine over 24 hours (•••), measured cumulative acetaminophen-glucuronide conjugates excreted in urine over 24 hours (O), and simulated cumulative acetaminophen-glucuronide conjugates excreted in urine over 24 hours (▬▬) for humans at various oral doses of acetaminophen (25). (B) Measured cumulative NAPQI conjugates excreted in urine over 24 hours (●) and simulated cumulative NAPQI pathway conjugates excreted in urine over 24 hours (▬ ▬ •) for humans at various oral doses of acetaminophen (25).
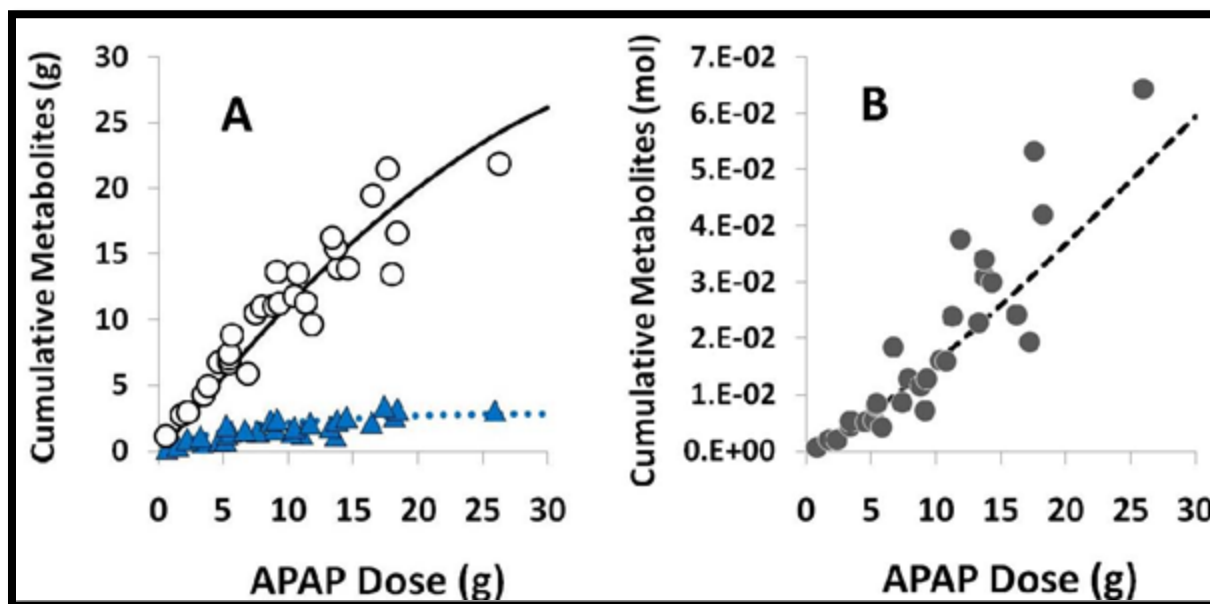
The critical aspect of Figure 2 is the dose response. The data and the simulation results cover a full range of acetaminophen doses, from subtherapeutic doses through large overdoses. This shows that DILIsym accurately predicts the metabolism elimination pathways for acetaminophen across a wide dosing range. The metabolism component of the PBPK model is the most important aspect for acetaminophen due to

the NAPQI metabolite being the primary driver of toxicity at exposures that deplete glutathione. In addition to metabolism, the human acetaminophen PBPK model has also been extensively validated with plasma data (26–29), a sampling of which is shown below in Figure 3.

Figure 3 - Select human acetaminophen PK data (black circles) from a variety of studies (26–28) and dosing routes compared to DILIsym simulation results (lines); figure continued on next page
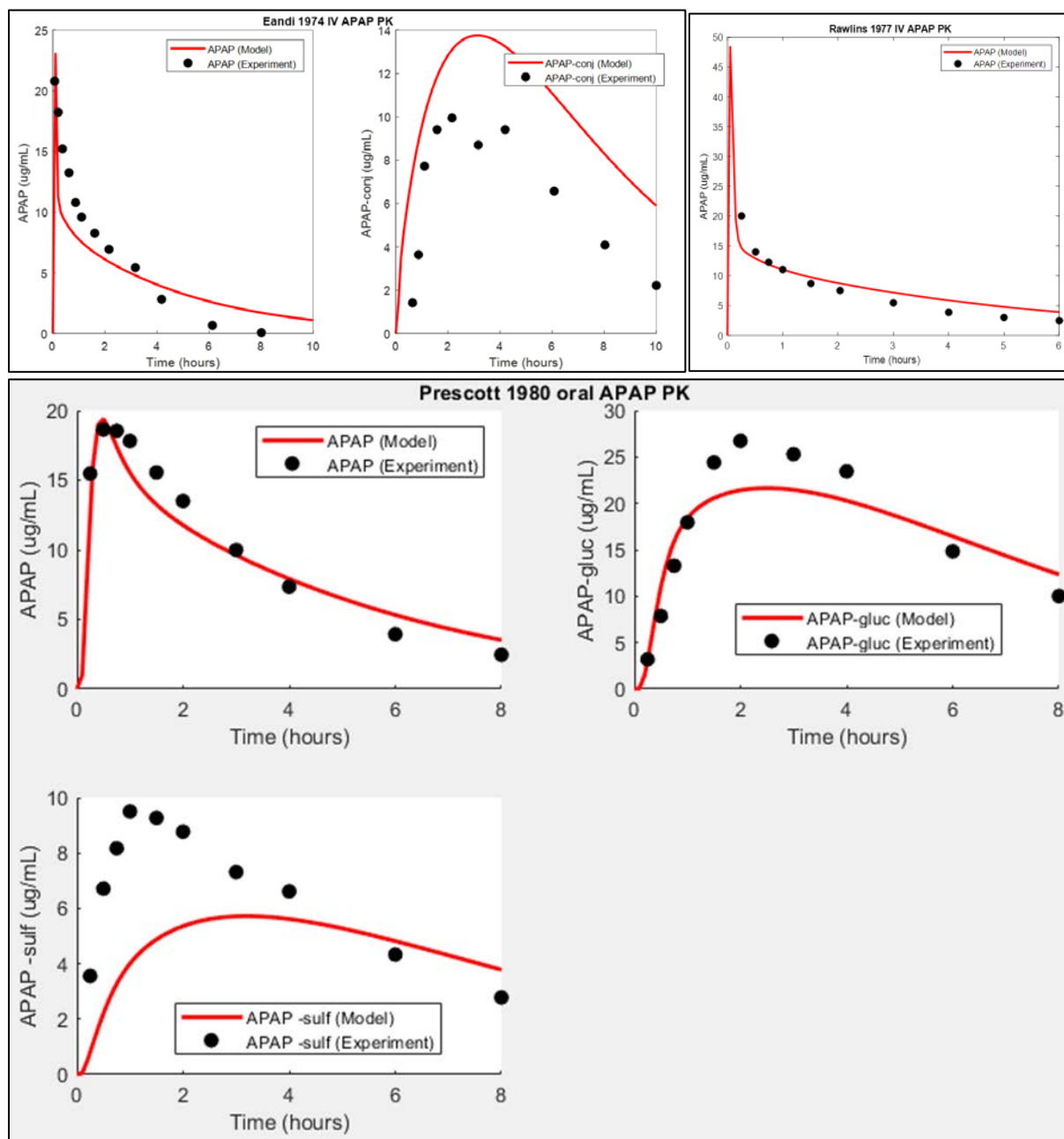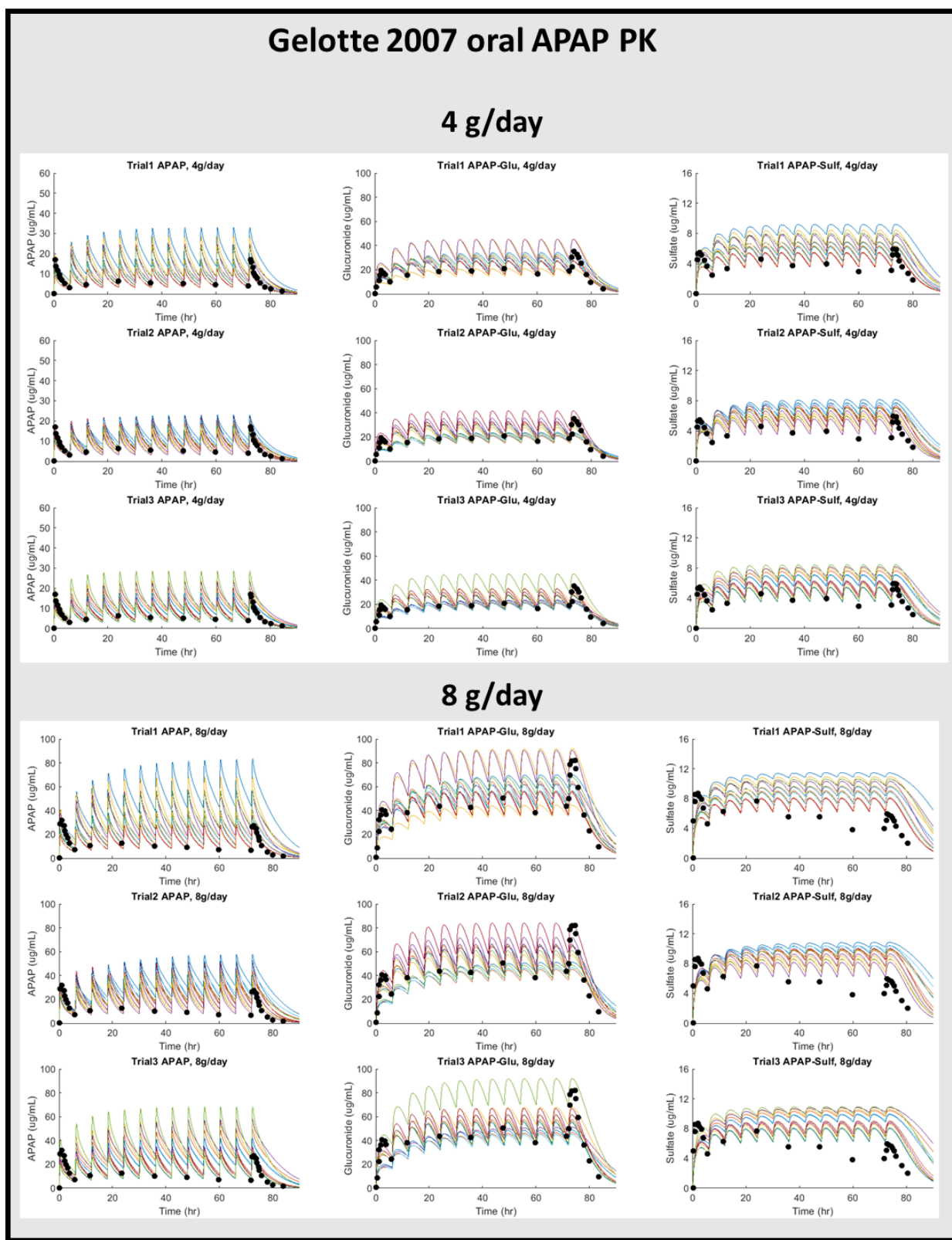
Figure 3 *continued* (29)

Gelotte 2007 oral APAP PK

4.2 Human validation of biomarkers and mechanistic endpoints of toxicity

Singer 1995 (30) measured AST over time for a large number of acetaminophen overdose patients taking an average of about 30 g of acetaminophen, although doses varied. DILIsym simulations for the average human compare well with the data, as shown in Figure 4.

Figure 4 - AST Measures Over Time for acetaminophen Overdose Patients by Singer 1995 (30)
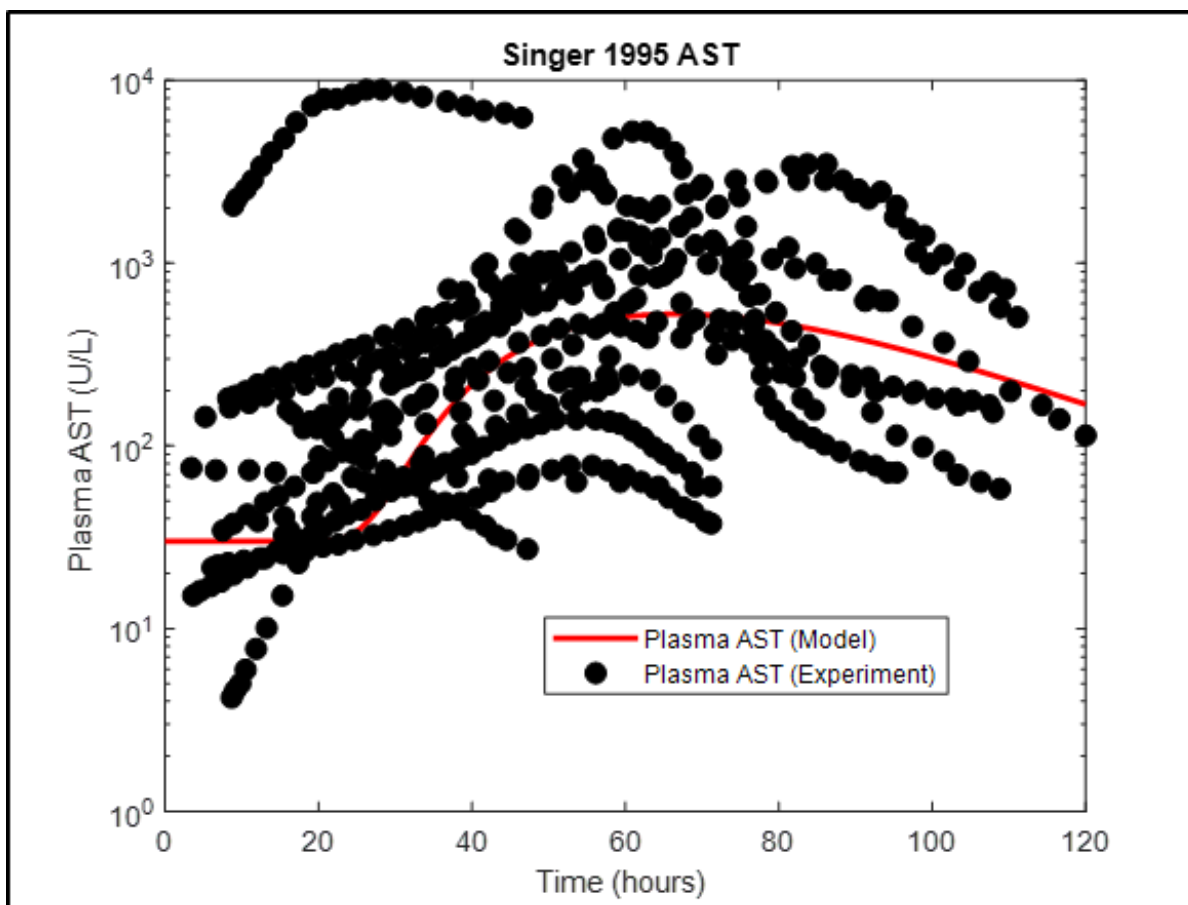
Watkins 2008 (31) measured hepatic alanine aminotransferase (ALT) in healthy subjects taking therapeutic doses of acetaminophen. DILIsym predicts these very minor but present ALT elevations even at low doses, showing that DILIsym correctly represents the full acetaminophen dose response (Figure 5).

Similarly, Temple 2007 (29,32) measured ALT in subjects taking therapeutic (4 g/day) and supratherapeutic (6 g/day and 8 g/day) doses of acetaminophen (Figure 5). In this study, urinary recovery of total thiols, which are the metabolites of NAPQI-GSH conjugation, were also quantified (29). To recapitulate the acetaminophen metabolism involved in formation of the NAPQI reactive metabolite in these subjects, DILIsym simulations were performed in three sets (i.e., trials) of twelve simulated individuals matching urinary recovery of thiols in each study group. DILIsym predicted no ALT elevations above the upper limit of normal for 4 g/day for all three trials, consistent with clinical data. At the acetaminophen dose of 6 g/day, no ALT elevations above the upper limit of normal were predicted in simulations of one set of 12 individuals, whereas mild ALT elevations were predicted in simulations of two sets of 12 individuals with low frequency. Overall, DILIsym simulation results are generally in agreement

with clinical data (32), which showed hepatic safety for acetaminophen at the dose of 6 g/day. At the acetaminophen dose of 8 g/day, no ALT elevations above the upper limit of normal were predicted in simulations of two sets of 12 individuals, consistent with the clinical data. DILIsym simulations predicted an ALT elevation above 3X upper limit of normal in one set of 12 individuals, but the frequency was low (1 out of 12 individuals). Overall, DILIsym simulations recapitulate the hepatic safety of acetaminophen at the acetaminophen dose of 8 g/day (Figure 5).

Figure 5 - Low Dose acetaminophen Clinical Studies evaluating the plasma ALT elevations in a sensitive population at therapeutic doses (31) and in populations matching urinary recovery of thiols at therapeutic and supratherapeutic doses (29,32); figure continued on next two pages

Figure 5 continued (29,32)

Gelotte Group I

Clinical data (4 g/day) — **Simulation (4 g/day)**

Clinical data (6 g/day) — **Simulation (6 g/day)**

Total Thiols (% Recovery in urine)			
4 g/day		6 g/day	
Clinical data	Simulation	Clinical data	Simulation
	Trial 1: 9.3 ± 2.4		Trial 1: 10.2 ± 2.7
10.24 ± 3.91	Trial 2: 8.9 ± 2.3	9.75 ± 4.83	Trial 2: 10.1 ± 2.9
	Trial 3: 9.1 ± 2.4		Trial 3: 9.9 ± 2.5

Figure 5 continued (29,32)

Gelotte Group II

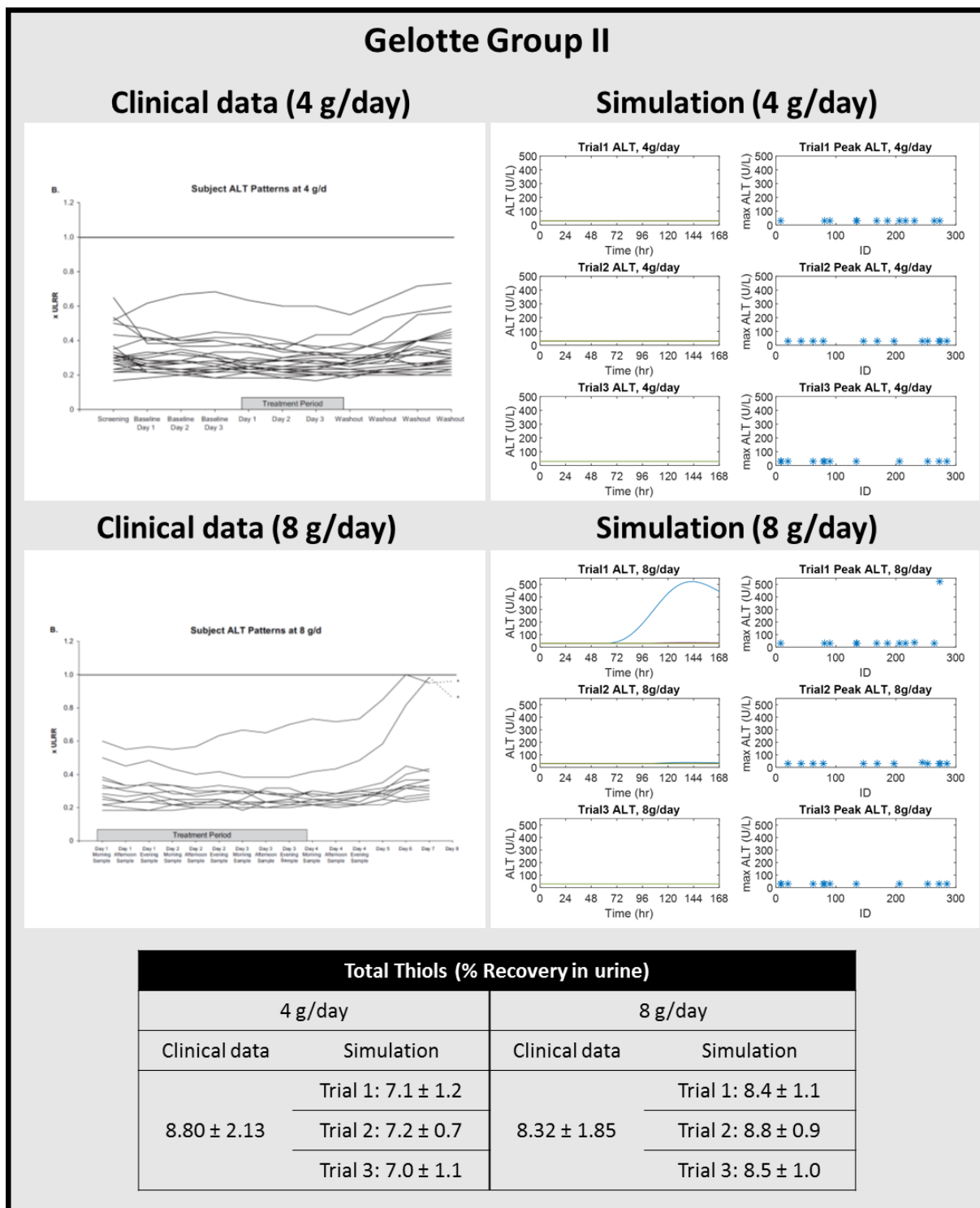| Total Thiols (% Recovery in urine)			
4 g/day		8 g/day	
Clinical data	Simulation	Clinical data	Simulation
8.80 ± 2.13	Trial 1: 7.1 ± 1.2	8.32 ± 1.85	Trial 1: 8.4 ± 1.1
	Trial 2: 7.2 ± 0.7		Trial 2: 8.8 ± 0.9
	Trial 3: 7.0 ± 1.1		Trial 3: 8.5 ± 1.0

Dixon 1992 (33) assessed AST and bilirubin for a number of acetaminophen overdose patients with MRI. The trends in those markers match up very well with the red simulated results. Even more intriguing and important, Dixon 1992 also measured liver ATP changes via MRI. The DILIsym predictions for ATP match up reasonably well (Figure 6), even though this was a blind prediction after DILIsym was fully developed and calibrated. The ATP data provide strong mechanistic validation for the DILIsym predictions of liver mitochondrial function and dysfunction as dose increases.

Figure 6 - Comparison of DILIsym predications compared to data for mitochondrial dysfunction as measure by ATP changes in Human Livers via MRI As reported by Dixon 1992 (33)
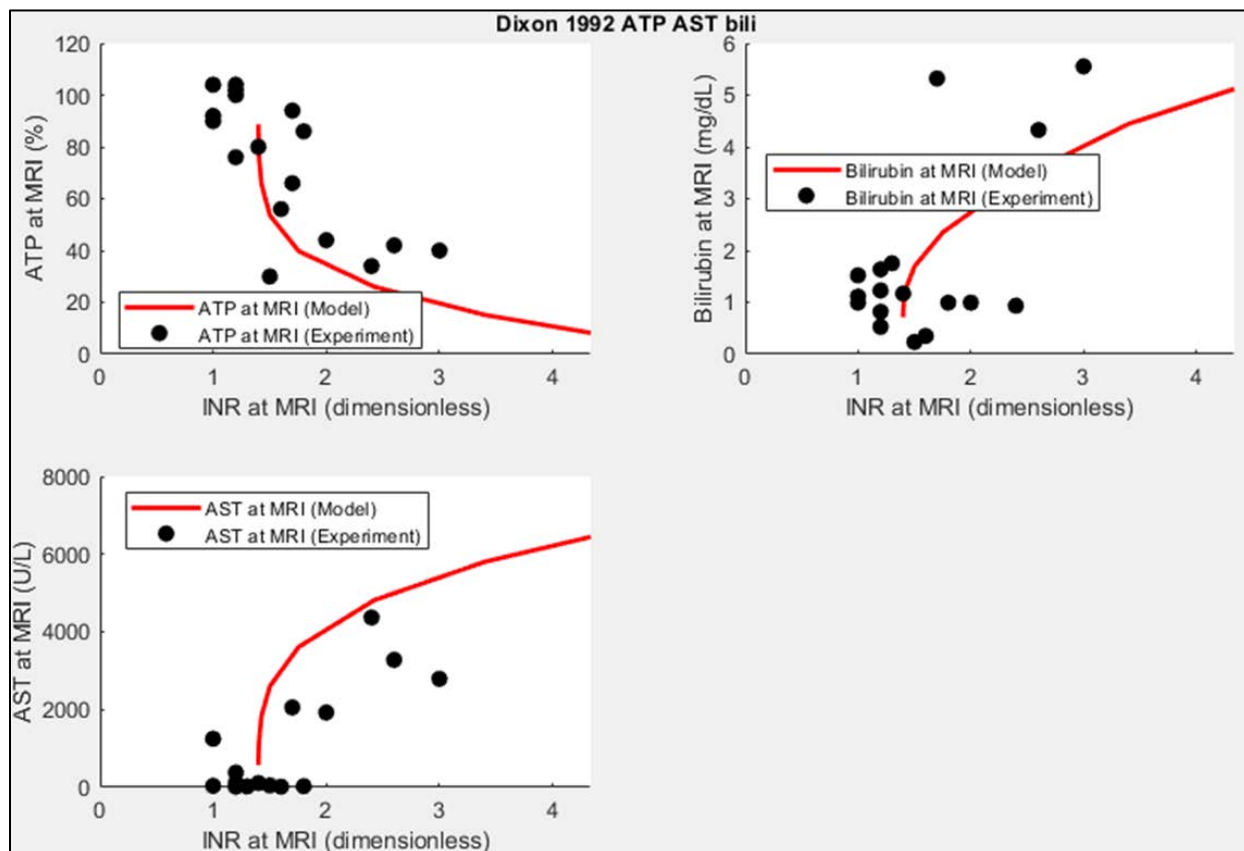
A critical aspect of acetaminophen injury is the subsequent repair that takes place. The human liver regenerates after this type of acute injury to pre-injury or near pre-injury levels over 3-12 months, with much of the regeneration taking place in the nearer term. A comparison (Figure 7) of the DILIsym liver regeneration rates after various doses of acetaminophen and various data sets, including the Portmann 1975 acetaminophen study (34) and many other liver surgery studies (35–39), shows very clearly that DILIsym is accurate and validated for predicting liver recovery from acetaminophen injury, as well as from acute liver injury in general.

Figure 7 - Simulated Liver Recovery Compared to Measured Liver Recovery After Liver Surgery or Acute acetaminophen Injury compared to experimental data (34–39).
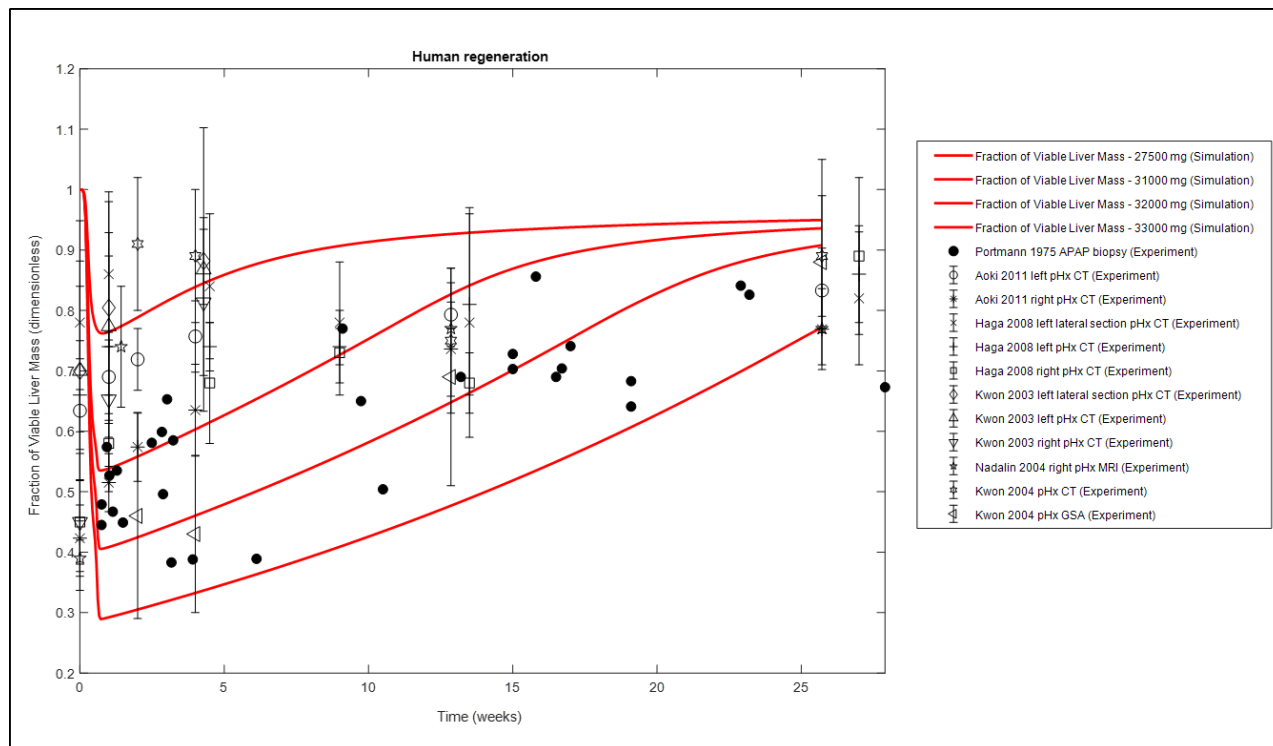
The data sets above represent a subset of the clinical validation data available for the acetaminophen representation in DILIsym. ***The data shown above demonstrate that the platform is sufficiently validated and able to support simulations of acetaminophen exposure-response for cellular effects and liver injury process in humans.***

4.3 Rodent validation of the physiologically-based pharmacokinetic model of acetaminophen and metabolites at various doses

Figure 8 shows published simulations and experimental results for rats and mice dosed with acetaminophen. The two figure panels show that DILIsym accurately captures the pharmacokinetics of acetaminophen as well as the production and clearance of its metabolites. Rats and mice have different metabolic profiles for acetaminophen, and DILIsym simulates these differences correctly.

Figure 8: Selected pharmacokinetic data used to optimize the APAP metabolism sub-model for rodents (mice and rats), shown with the corresponding simulation results produced with the DILIsym model *(1)*.

A) *Plasma APAP concentration data (◆), simulated plasma APAP concentration (▬ ▬ ▪), plasma APAP-sulfate concentration data (▲), simulated plasma APAP-sulfate concentration (• • •), plasma APAP-glucuronide concentration data (◯), simulated plasma APAP-glucuronide concentration (▬▬▬) for C57Bl/6 mice dosed via oral gavage with 300 mg/kg APAP. Mean and SD shown (1) .*

B) *Plasma APAP concentration data (◆), simulated plasma APAP concentration (▬ ▬ ▪), plasma APAP-sulfate concentration data (▲), simulated plasma APAP-sulfate concentration (• • •), plasma APAP-glucuronide concentration data (◯), simulated plasma APAP-glucuronide concentration (▬▬▬) for Sprague-Dawley rats dosed intravenously with 300 mg/kg APAP* (40).
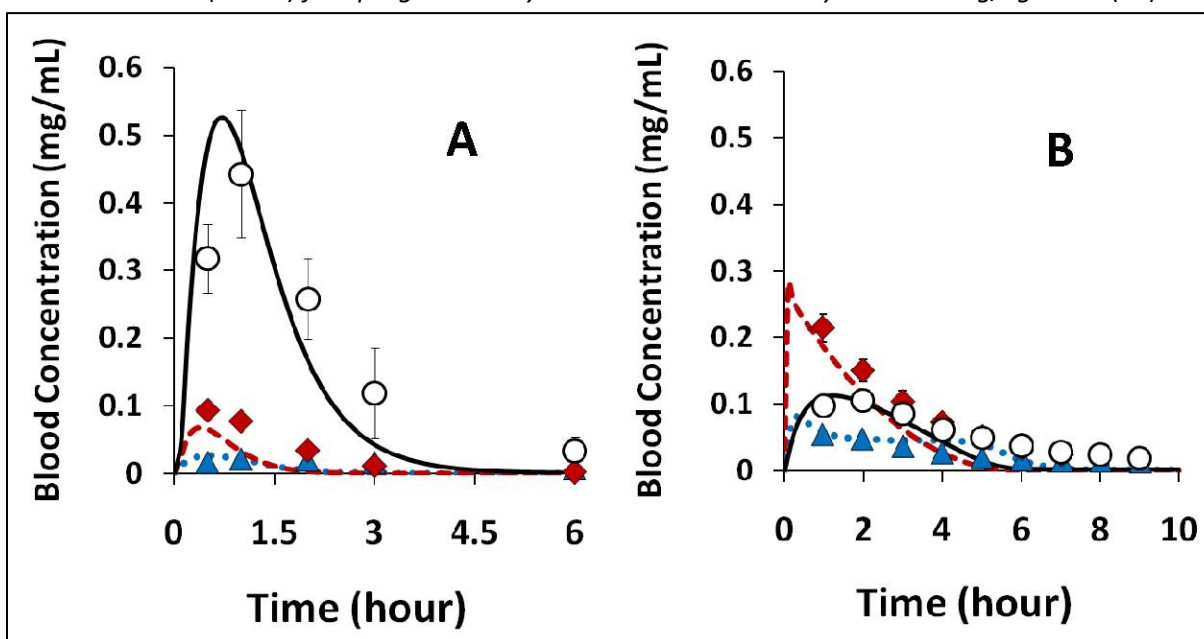
To illustrate DILIsym's ability to recapitulate pharmacokinetics for a range of doses of acetaminophen in rodents, Figure 9Figure 9 shows simulations versus rata data for plasma acetaminophen across a wide dosing range (41).

Figure 9: Simulated and measured APAP plasma levels in rats in doses ranging from 37.5 mg/kg to 600 mg/kg. Data from Hjelle 1984 *(41)* and simulations from DILIsym.
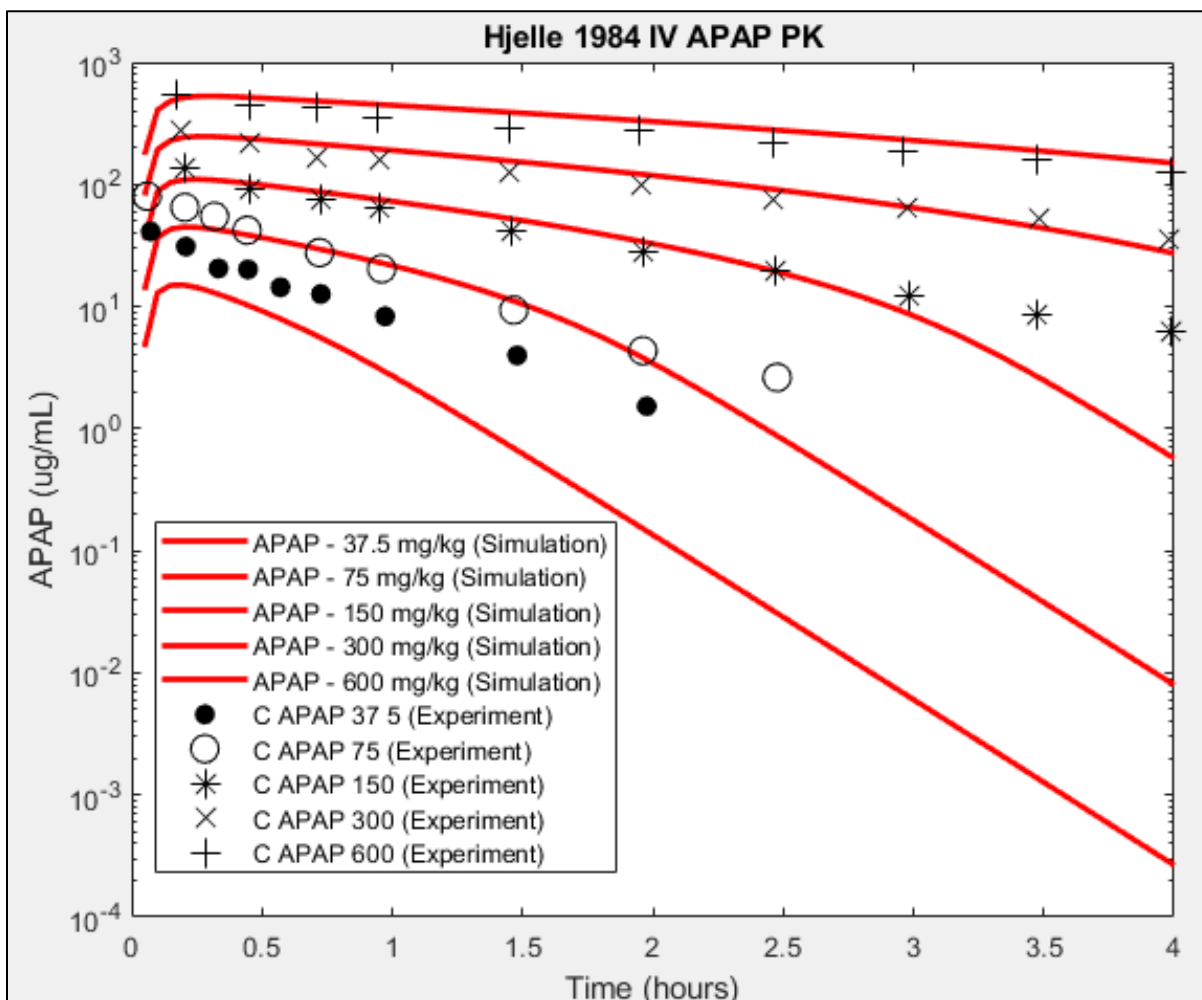
4.4 Rodent validation of biomarkers and mechanistic endpoints of toxicity

DILIsym has been extensively validated with respect to prediction of mechanistic and outcomes-related endpoints in rodents. Figure 10 shows good agreement between simulated and measured (42–49) GSH depletion in mice given 300 mg/kg of acetaminophen. The dynamic response, including GSH repletion, is well-captured within DILIsym.

Figure 10: GSH depletion and repletion in mice given 300 mg/kg predicted by DILIsym (red line) and measured in mice (symbols) *(42–49).*
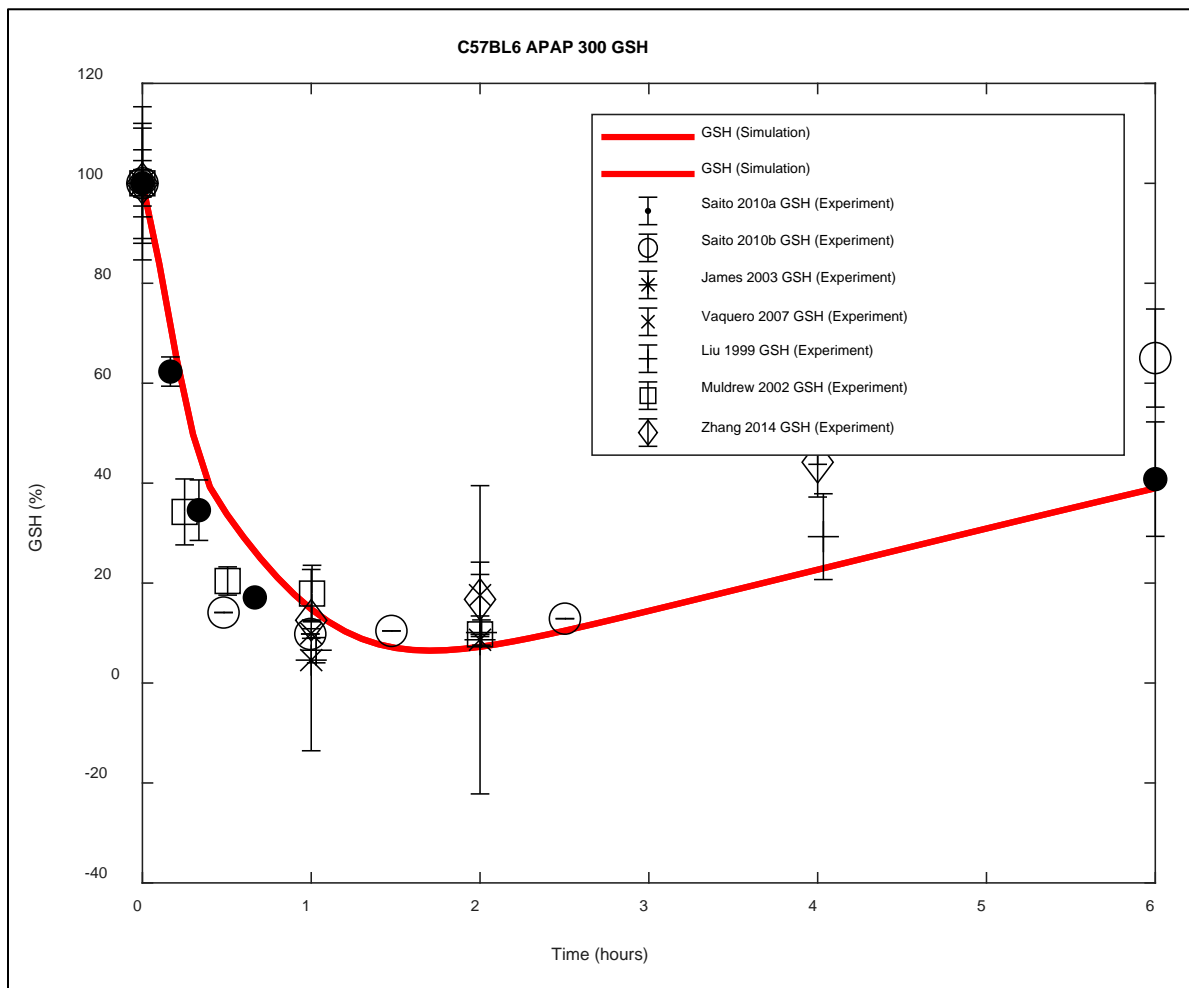
GSH depletion in rats, along with rapid repletion upon dosing of N-acetylcysteine (NAC), is shown in Figure 11(50). DILIsym correctly simulates both the control (APAP) and treated (APAP + NAC) cases.

Figure 11: GSH depletion and repletion through treatment with NAC in rats as a function of time, both simulated (red lines) and measured *(50).*
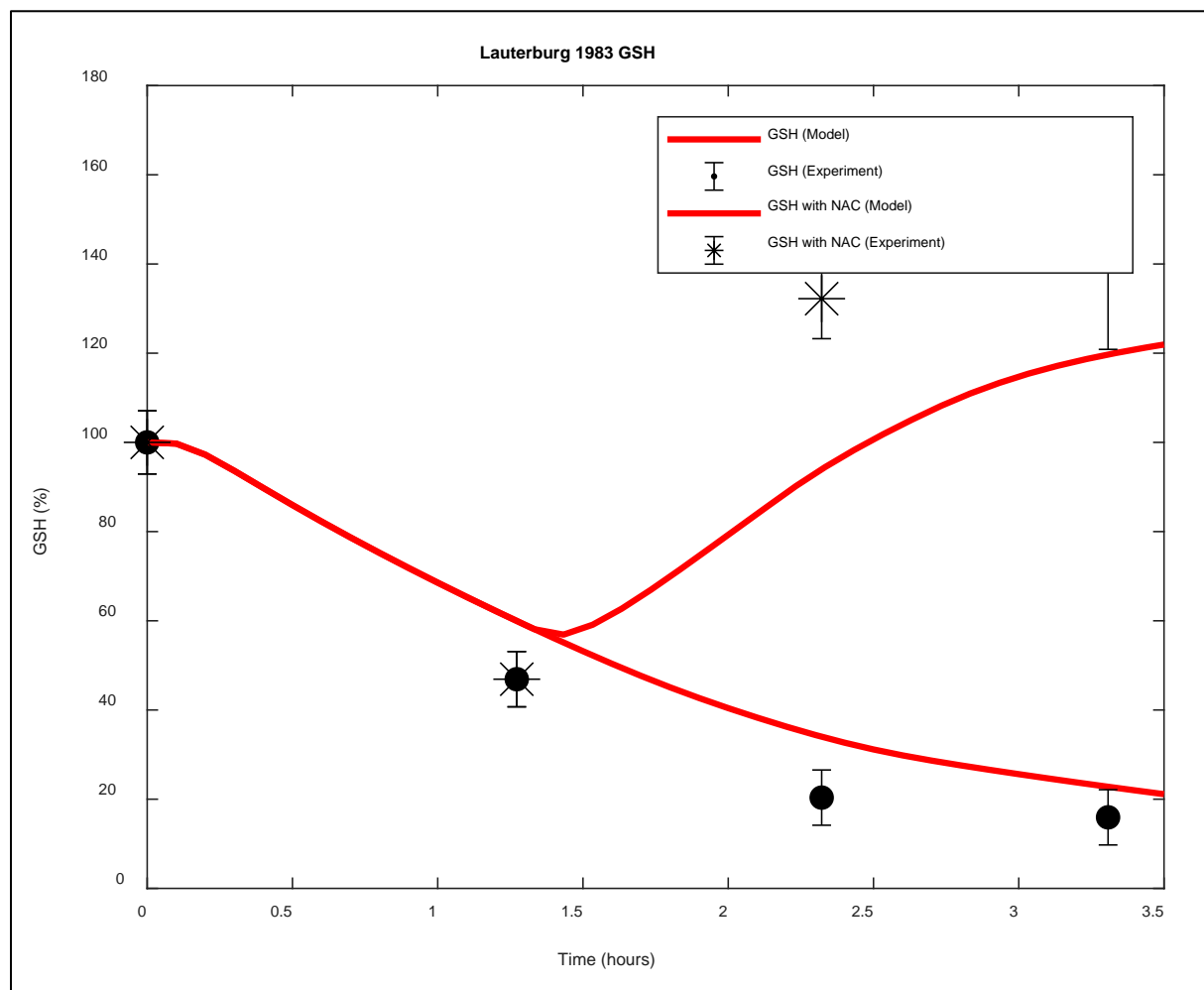
In addition to predicting GSH dynamics in rodents, DILIsym was also designed to simulate protein adducts produced in the liver when acetaminophen is administered to rodents at high doses. Figure 12 to Figure 14 for rats (51), mice (46), and mice (48) show liver protein adducts (Figure 12), liver GSH (Figure 13) and protein adducts (Figure 14), and liver protein adducts + plasma protein adducts + liver GSH, respectively. In all cases, the simulations (red lines) line up reasonably well with the measured data.

Figure 12: Liver protein adduct levels in rat livers versus time after APAP dosing from DILIsym (red line) and measured *(51)*.
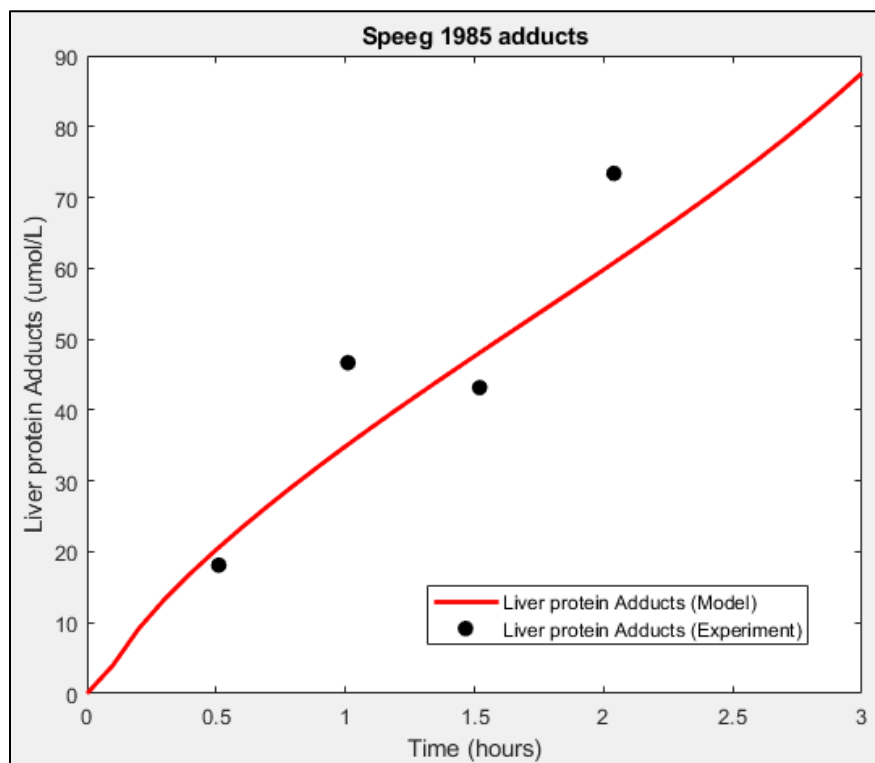
Figure 13: Liver GSH and protein adducts from Vaquero 2007 (mouse) *(46)* and simulated (red lines).
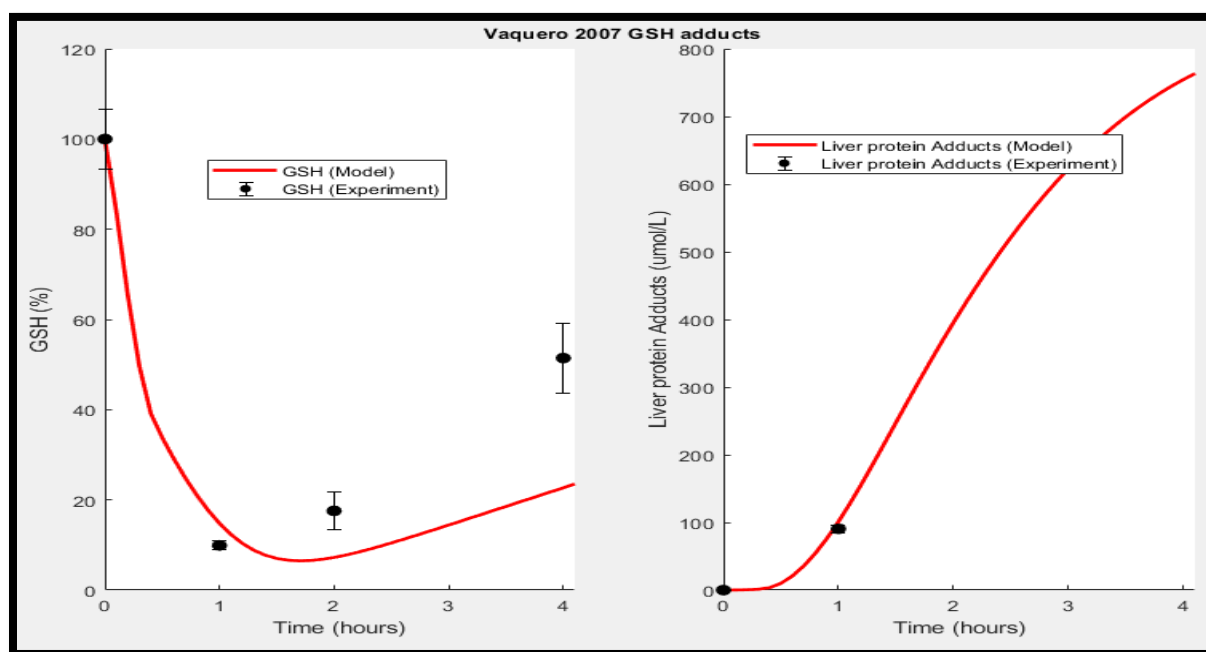
Figure 14: Liver protein adducts + plasma protein adducts + liver GSH from Muldrew 2002 (mouse) *(48)* and simulated (red lines).
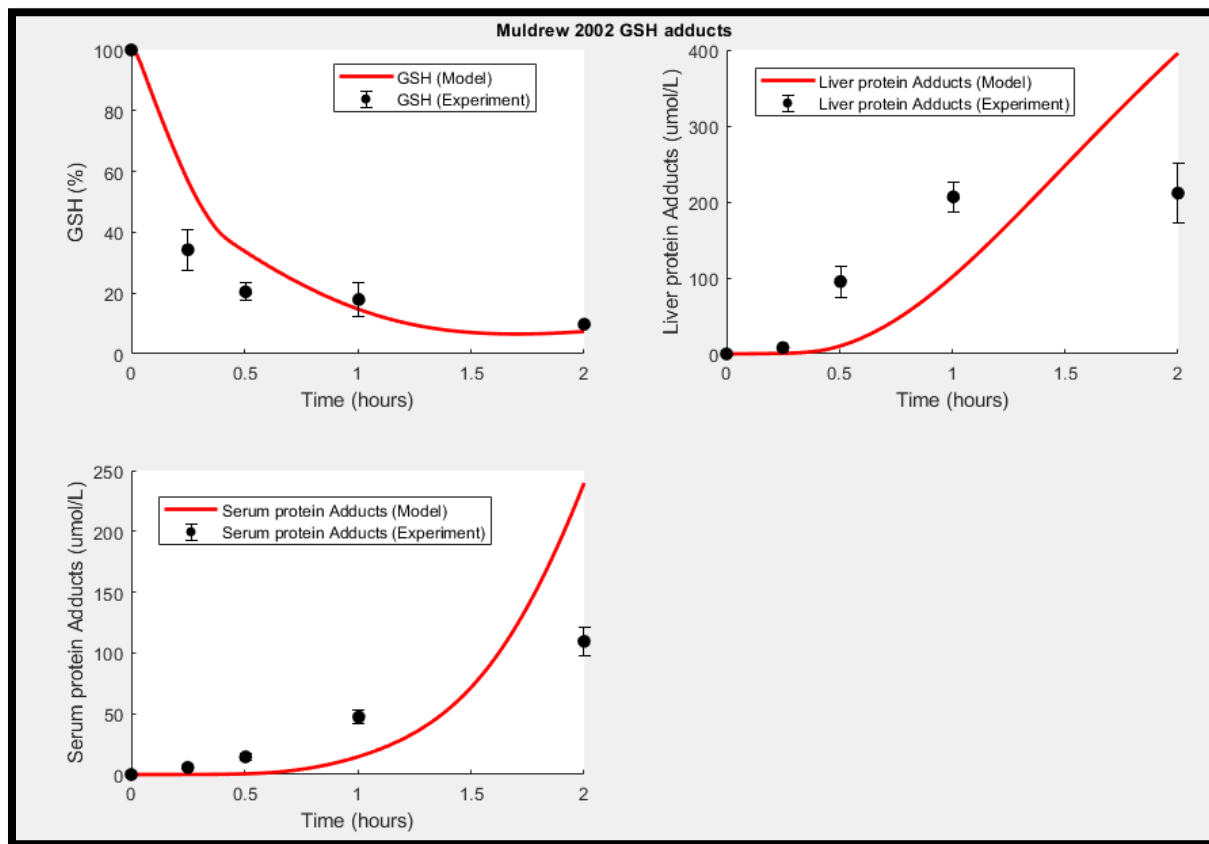
A critical part of the acetaminophen liver toxicity pathway involves mitochondrial function impairment. DILIsym is capable of simulating the kinetic changes in liver ATP as the acetaminophen dose increases in both mice and rats. This change in ATP occurs due to an inhibition of ATP production in the liver. Figure 15 and Figure 16 show that DILIsym represents the drop in liver ATP with increasing acetaminophen dose reasonably well in rodents.

Figure 15: Liver ATP versus time in mice from a number of studies *(52–55)* and simulated (red lines) by DILIsym across a dose range of 100 mg/kg to 600 mg/kg.
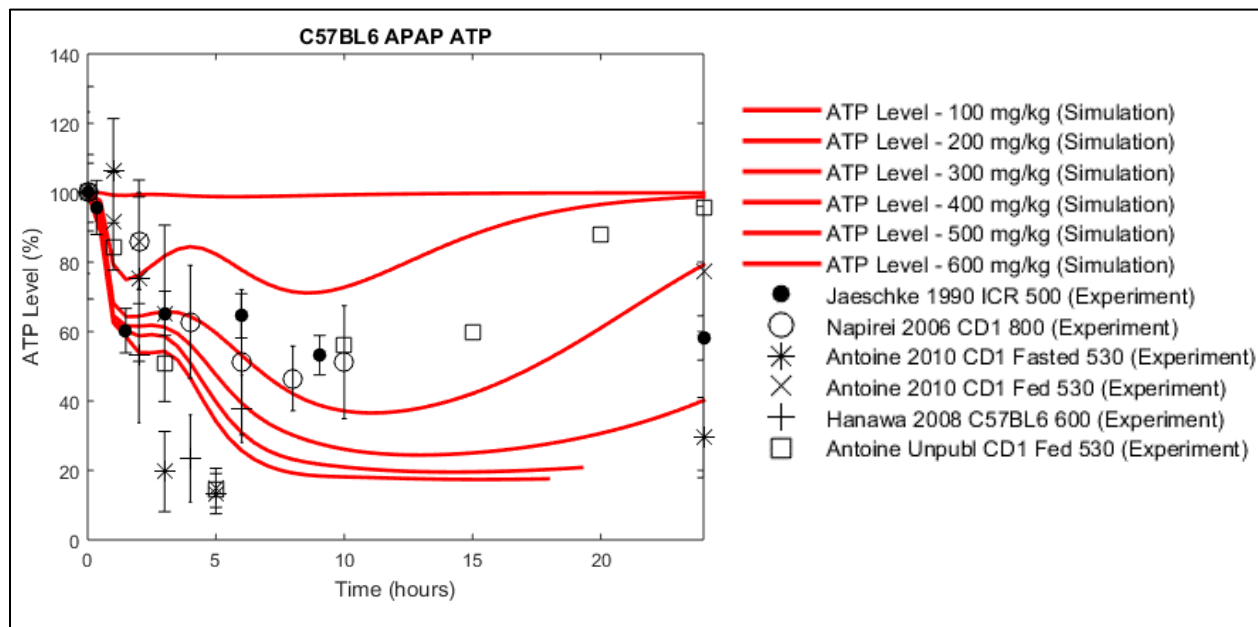
Figure 16: Liver ATP versus time in rats from a number of studies *(56–59)* and simulated (red lines) by DILIsym across a dose range of 800 mg/kg to 1500 mg/kg.
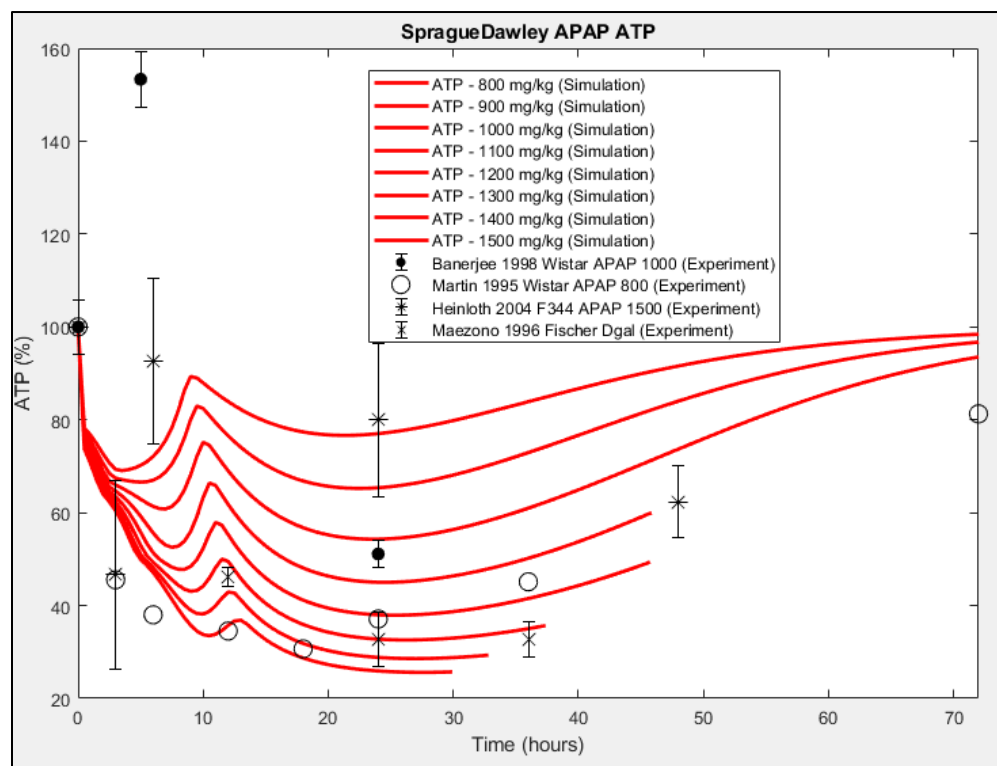
The ultimate outcome of the reactive metabolite production from acetaminophen, the drop in GSH, and the impairment of ATP production is cell death. This leads to liver enzyme spillage. Figure 17 and Figure 18 below show ALT versus APAP dose in mice and rats from DILIsym and a large number of preclinical studies. While the data is extremely variable across different studies, DILIsym does a reasonable job of recapitulating the dose response. The mouse and rat SimPops with variability within DILIsym have simulated animals with variability in sensitivity as well.

Figure 17: ALT versus APAP dose from various mouse studies *(45,60–76)* and DILIsym (red lines).
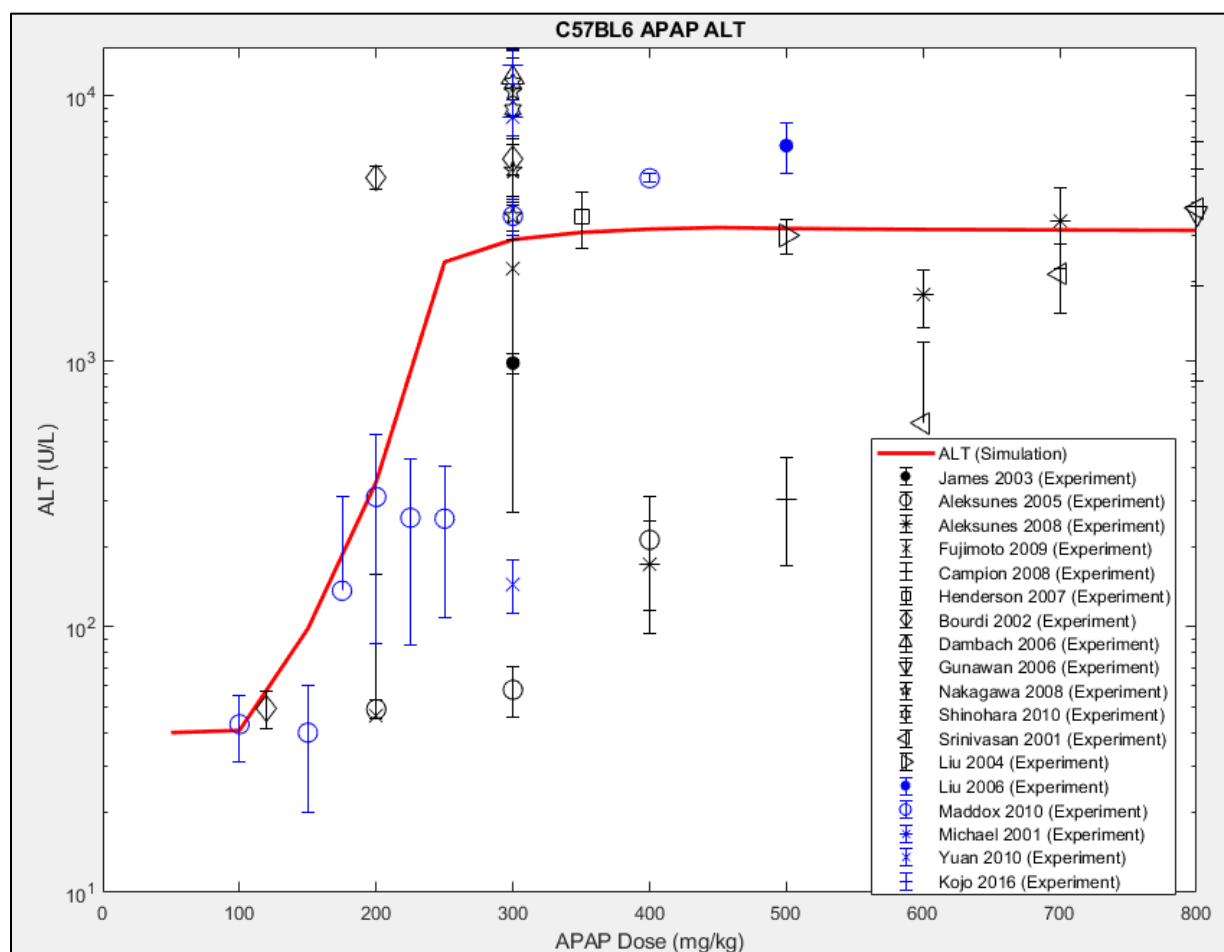
Figure 18: ALT versus APAP dose from various rat studies *(57,77–87)* and DILIsym (red lines).
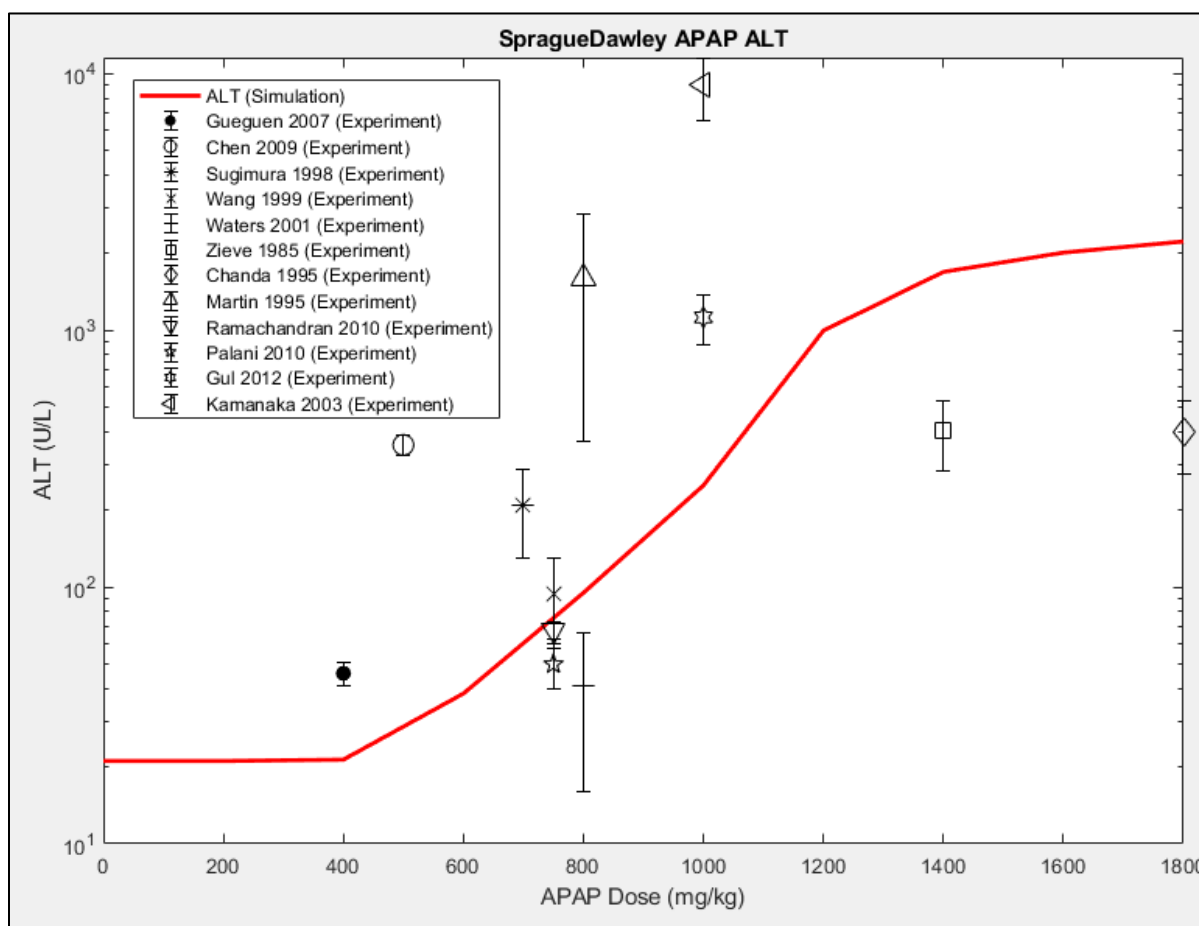
With an emphasis on clinical acetaminophen within this work, not all rodent validation data is included. However, there is a large battery of very mechanistic and preclinical biomarker data supporting the DILIsym representations for mice and rats available in the primary and supplemental text of the following publications: (1–3). Readers are highly encouraged to review the referenced DILIsym acetaminophen publications to see the full scope of the validation of DILIsym for representing acetaminophen accurately across species.

5   Simulation of the Acetaminophen Liver Toxicity Pathway Shows that its Mode of Action Precludes it from Being a Carcinogenic Hazard

For this analysis of acetaminophen, thousands of unique human scenarios were simulated that were comprised of a) unique simulated individuals with variability in underlying biochemical and functional pathways including phenotypic variation in metabolism (DILIsym SimPops "*Human_APAP_ROS_apop_mito_v3B_2"* comprised of 300 simulated humans) and b) different dosing schemes including low, medium, and high doses. A database of simulation results from this series of simulations was compiled, allowing us to visualize the steps involved in the acetaminophen hepatotoxicity pathway and how those steps relate to the key characteristics that have been attributed to increased risk for carcinogenicity, including reactive molecules and ROS. The simulated results were compared to animal and human data where available.

5.1   Sequence of Events in Acetaminophen MOA Pathway

The sequence of events occurring along the acetaminophen toxicity pathway can be viewed as a time-course at a given dose level or based on the dose/exposure-response. Starting with the kinetic perspective, the top half of Figure 19 shows that at therapeutic doses GSH levels are slightly reduced but there is sufficient capacity to bind up all of the NAPQI. The bottom half of Figure 19 shows how following a 20 g overdose of acetaminophen per day for 1 week, GSH is depleted within a day, and then ROS, NAPQI-protein adducts, and mitochondrial impairment increase in parallel.

Figure 19: Kinetic view of acetaminophen Effects in Liver Under Therapeutic and Overdose Conditions (Subject 298 from the SimPops of 300)

APAP QID Dosing for 1 Week at 2 Doses in Single Simulated Individual
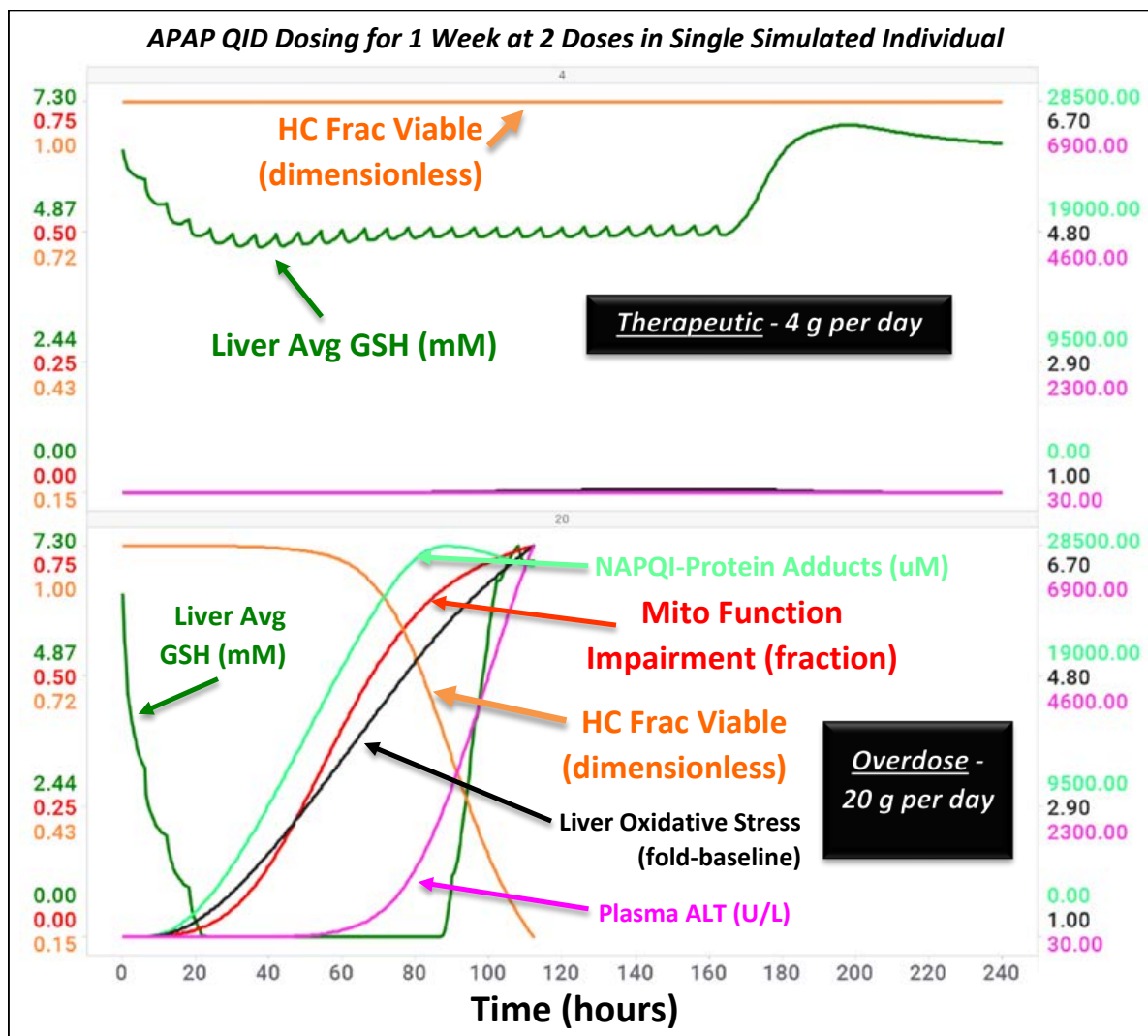
See Table 1 for validation summary of each of these endpoints with DILIsym

Cell death occurs shortly after these events, as there is a slight delay for cells to die once ATP production is reduced. This simulated sequence shows that acetaminophen liver toxicity is binary from a kinetic standpoint – once GSH is depleted and the effective buffer for NAPQI conjugation is gone, mitochondrial dysfunction drives oxidative stress and cell death, and subsequent repair through regeneration of hepatocytes occurs. The kinetics of acetaminophen injury in the liver have been studied in animals (48) (Figure 20), and the results support the simulated depiction of the event in humans in Figure 19 as reasonable.

Figure 20: Mice treated with acetaminophen at a hepatotoxic dose of 300 mg/kg i.p. (n = 5) and were sacrificed at designated times. Samples of liver were analyzed for acetaminophen-CYS and GSH and the time course for APAP-CYS increase matches the time course for the decrease in liver GSH (Muldrew 2002 (48))
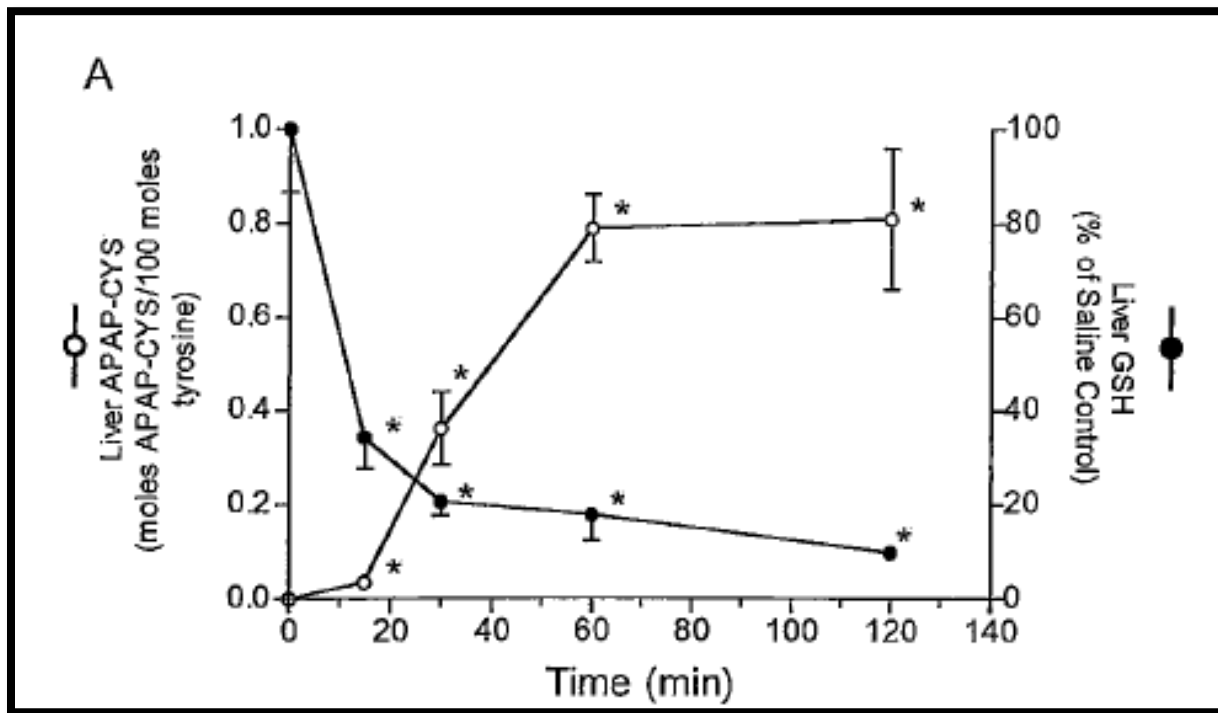
The reduction in liver GSH within the mouse study is very much coincident with the increase in covalent binding, which is in good agreement with the simulated overdose case of 20 g per day in Figure 19.

The sequence of events within the acetaminophen MOA for toxicity can also be viewed through from an exposure-response perspective, as shown in Figure 21. The figure highlights the events in the centrilobular region of the liver specifically, which should be noted since that zone is the most sensitive to acetaminophen toxicity. In the small centrilobular region of the liver that is most sensitive to acetaminophen due to the presence of more CYP450 metabolizing enzymes in that zone, single doses up to about 10 g of acetaminophen produce minimal ROS and still leave adequate GSH buffer. Beyond 10 g, ROS and mitochondrial function impairment increase concurrently, with cell death again becoming evident through increased ALT with a slight delay. Last in the sequence of events is an increase in hepatocellular proliferation that provides repair of the damaged areas of the liver, assuming the dose is low enough for the liver damage to be less than a critical level, in which case the patient will survive and make a full recovery.

Figure 21: Acetaminophen Dose Escalation Simulations for Centrilobular Region of Liver
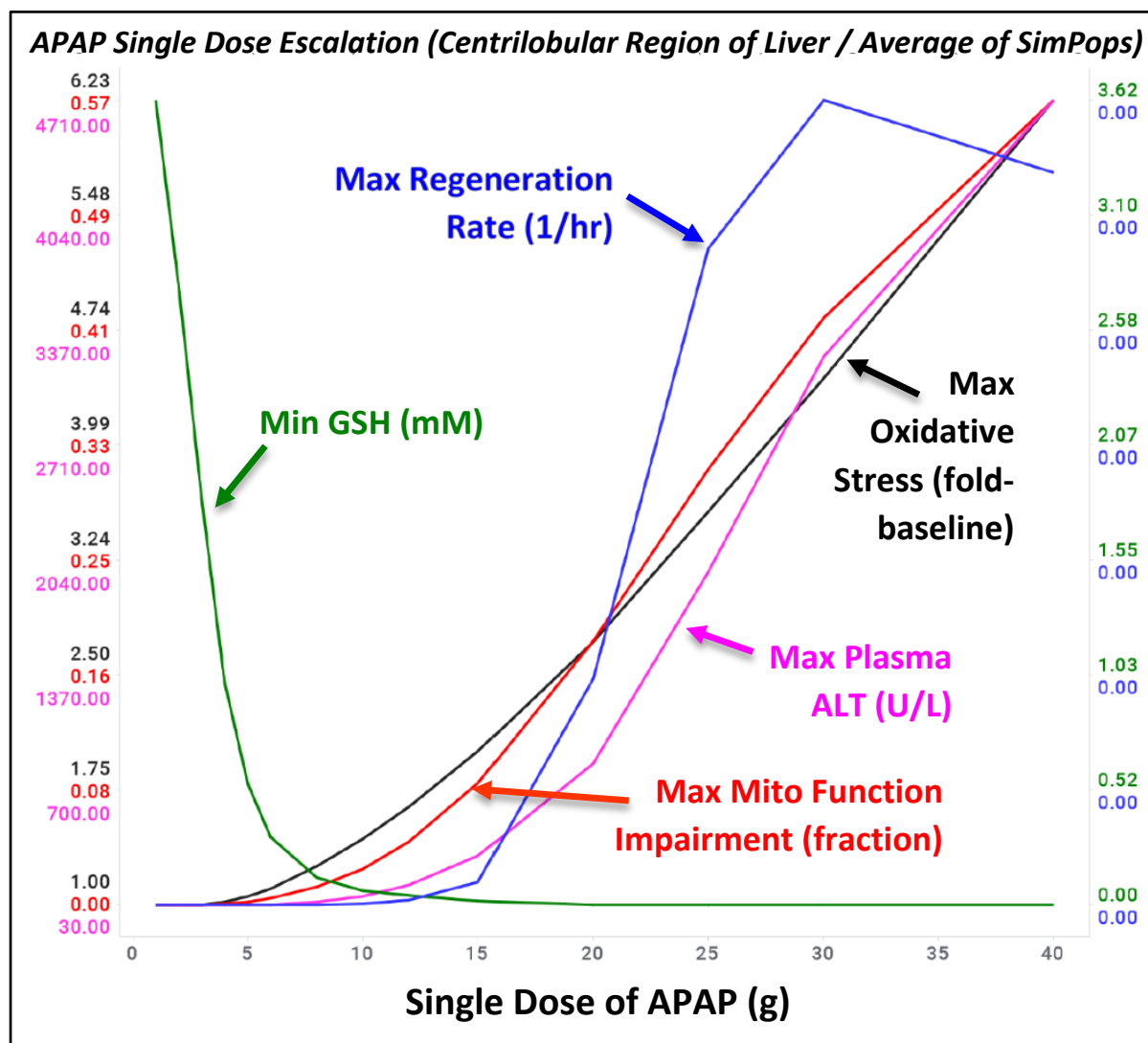
*See Table 1 for validation summary of each of these endpoints with DILIsym

The sequence can also be visualized across the entire liver in an exposure-response manner, with more endpoints as well (Figure 22). The normalized figure shows the sequence of events from an average liver standpoint, as opposed to a specific region or zone of the liver: acetaminophen exposure at clinically relevant doses causes minimal GSH depletion, minimal cell death, and minimal mitochondrial injury and ROS; acetaminophen exposure beyond this level (around approximately 10 g for the single dose case) leads to substantial GSH depletion, increases in NAPQI available to bind to various cellular targets, coincident mitochondrial function impairment and ROS, increases in NAPQI-protein adducts, cell death and associated biomarkers, and lastly, injury repair via hepatocellular regeneration.

Figure 22: Dose Escalation Simulations for the whole liver show that acetaminophen exposure at clinically relevant doses causes minimal GSH depletion, minimal cell death, and minimal mitochondrial injury and ROS. As acetaminophen exposure reach approximately 10 g for the single dose case, there is substantial GSH depletion, increases in NAPQI protein adducts, impaired mitochondrial function resulting in Reactive Oxygen Species (ROS) and cell death. Lastly, liver injury is repaired via hepatocellular regeneration. Since no DNA adducts have been structurally identified in vivo they are not considered in the modeling.
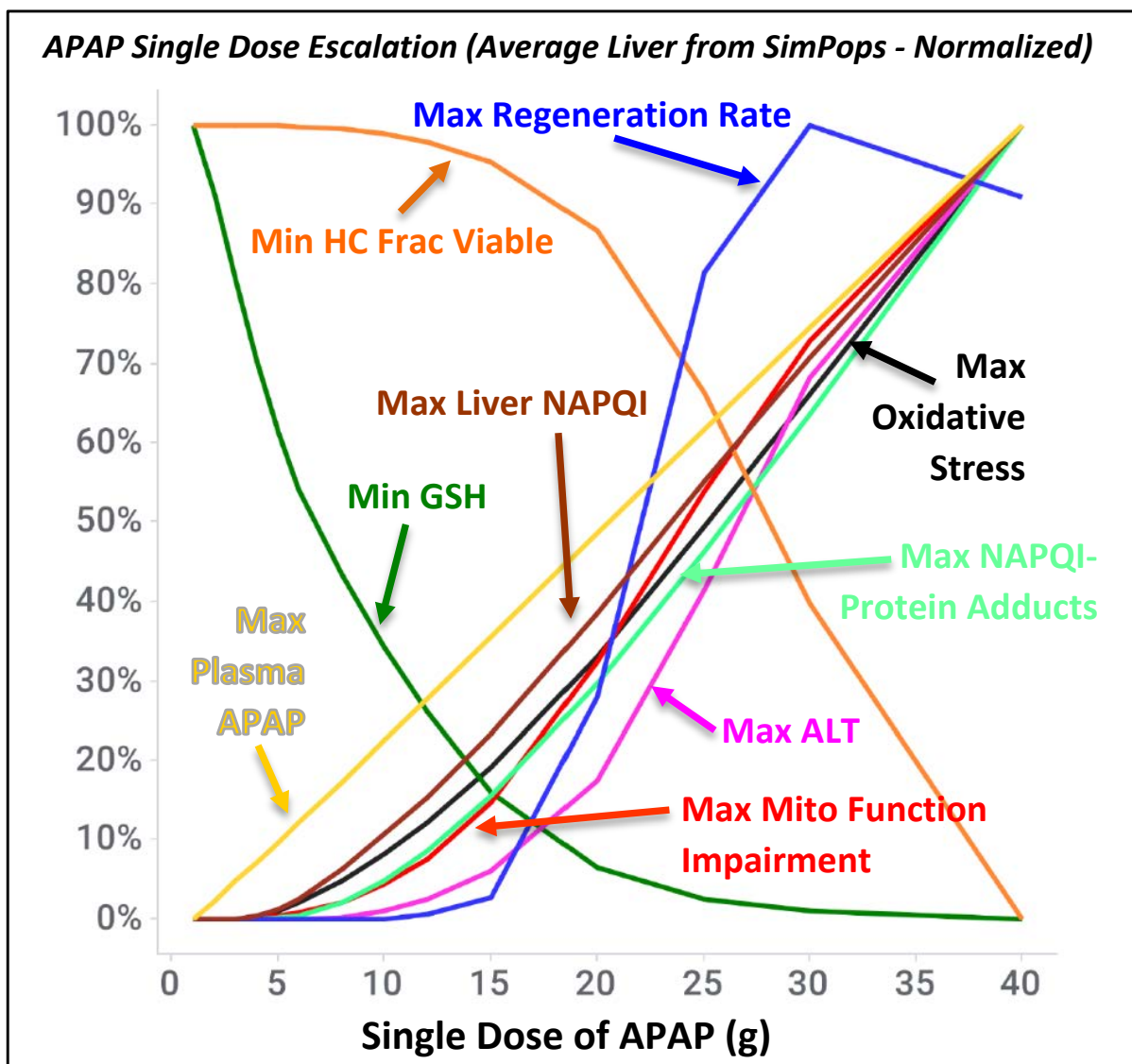
*See Table 1for validation summary of each of these endpoints with DILIsym

Beyond the extensive prior validation of the DILIsym software for representing and depicting the MOA, experimental evidence also exists (88) to support these simulated depictions of the acetaminophen MOA from an exposure-response standpoint. For example, Figure 23shows liver GSH and covalent binding as the acetaminophen dose increases in hamsters. NAPQI covalent binding increases sharply as GSH falls, in full qualitative agreement with the trends shown in Figure 21 and Figure 22.

Figure 23: Comparison of covalent binding of 3 H-acetaminophen in vivo to hamster hepatic protein (■) and hepatic glutathione depletion in hamster (o) 3 h after the intraperitoneal administration of varying doses of 3 H-acetaminophen. Each point represents the mean ± standard error of determinations in at least three hamsters. (Potter 1974 (88))
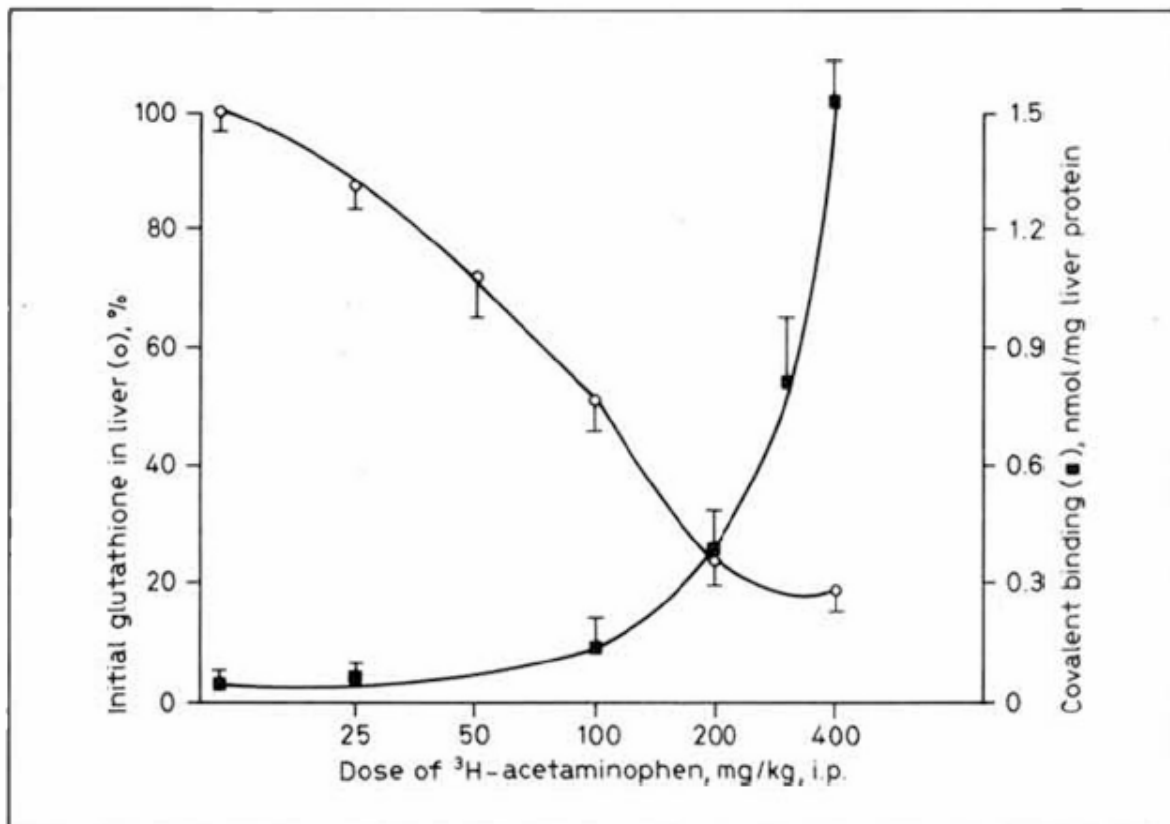
5.2 Lack of Key Characteristics of Carcinogenicity in Humans in the Absence of Toxicity

The 4 g per day time-course plot from Figure 19 shows that excess GSH buffer capacity leads to no ROS or mitochondrial function impairment in an average patient, as well as an absence of cell death. However, at the 20 g per day dosing level (bottom of Figure 19), the GSH buffer is wiped out and the sequence of events leading to toxicity occur. The two figures effectively illustrate a critical aspect of acetaminophen toxicity that precludes it from being carcinogenic: either ***excess buffer capacity through GSH and cytosolic proteins prevents any ROS or injury by de-activating the reactive NAPQI, or hepatocyte death occurs in the event of complete depletion of GSH. At no time in this sequence of events do material amounts of ROS get produced unless those cells die, and at no point does any nuclear DNA damage occur unless again, those cells die. Therefore, the reactive metabolites and ROS produced during this sequence, in the event of toxicity, do not fall under the heading of key characteristics of carcinogens, since they only appear coincident with cell death.***

The centrilobular liver region dose response simulation (Figure 21) also shows that the events associated with acetaminophen toxicity either do not occur due to the GSH buffer (therapeutic and supratherapeutic doses) or occur as a collective set of events associated with liver injury and cell death. *This narrow window between GSH being depleted and liver cell death is strong evidence for the lack of a dosing level where key*

characteristics of carcinogenicity occur for acetaminophen but without those same cells dying and then regenerating as healthy cells. Figure 22 provides further confirmation, where plasma acetaminophen values in the therapeutic range lead to minimal toxicity or stress. Furthermore, Figure 22 highlights that cell death starts right as the average liver GSH is depleted to 30% or less, exactly coincident with ROS increases, protein adduction, and mitochondrial dysfunction occurs.

In summary, acetaminophen is somewhat unique in that its MOA for toxicity leads to a very binary response: safe use at clinically relevant levels or liver injury at higher doses.

5.3   Population variability in GSH, Acetaminophen PK, and ROS Clearance

The simulated kinetics and dose-response of acetaminophen exposure in the average individual shown above clearly shows adequate buffer and protection from any ROS or un-mitigated reactive species at clinically relevant acetaminophen doses, with a narrow range for the conversion from this regime to a regime where ROS is generated, but is generated concurrent with mitochondrial toxicity and cell death that is marked by GSH depletion. However, it is important to understand whether or not this picture changes with population variability. The DILIsym acetaminophen SimPops contains variability in baseline liver GSH concentrations, GSH synthesis capability, ROS clearance, acetaminophen ADME processes (PK), body mass, and sensitivity for mitochondrial function impairment (Human_APAP_ROS_apop_mito_v3B_2 SimPops). The ranges for variability were taken from literature and are documented within the DILIsym software.

A myriad of acetaminophen dosing protocols was simulated in the SimPops containing 300 simulated humans. Figure 24 shows the population picture from a kinetic viewpoint at 4 g of acetaminophen per day and 12 g of acetaminophen per day over 1 week. The 4 g time-course shows adequate GSH buffer across the full population, with minimal effects on mitochondrial function and minimal hepatocyte death. Clearly, the actual clinical use case of acetaminophen does not subject patients to stress in their livers that would have any relevance for carcinogenicity, even when considering a wide range of patient types. On the other hand, the 12 g per day time-course in Figure 24 shows GSH depletion occurring in some members of the SimPops, which then leads to mitochondrial impairment and cell loss (slightly delayed since ATP levels have to drop over a period of time, which then causes cell death). The population-level Figure 24 outlines the close connection between GSH depletion, mitochondrial dysfunction, and cell death, and again highlights the key point: ***Acetaminophen exposure only results in significant oxidative stress or DNA effects under conditions that cause cell death. Simulations support this observation across a wide range of patient types and backgrounds.***

Figure 24: Kinetic Liver Effects of acetaminophen Simulated in Human SimPops of 300 Individuals at 2 Doses
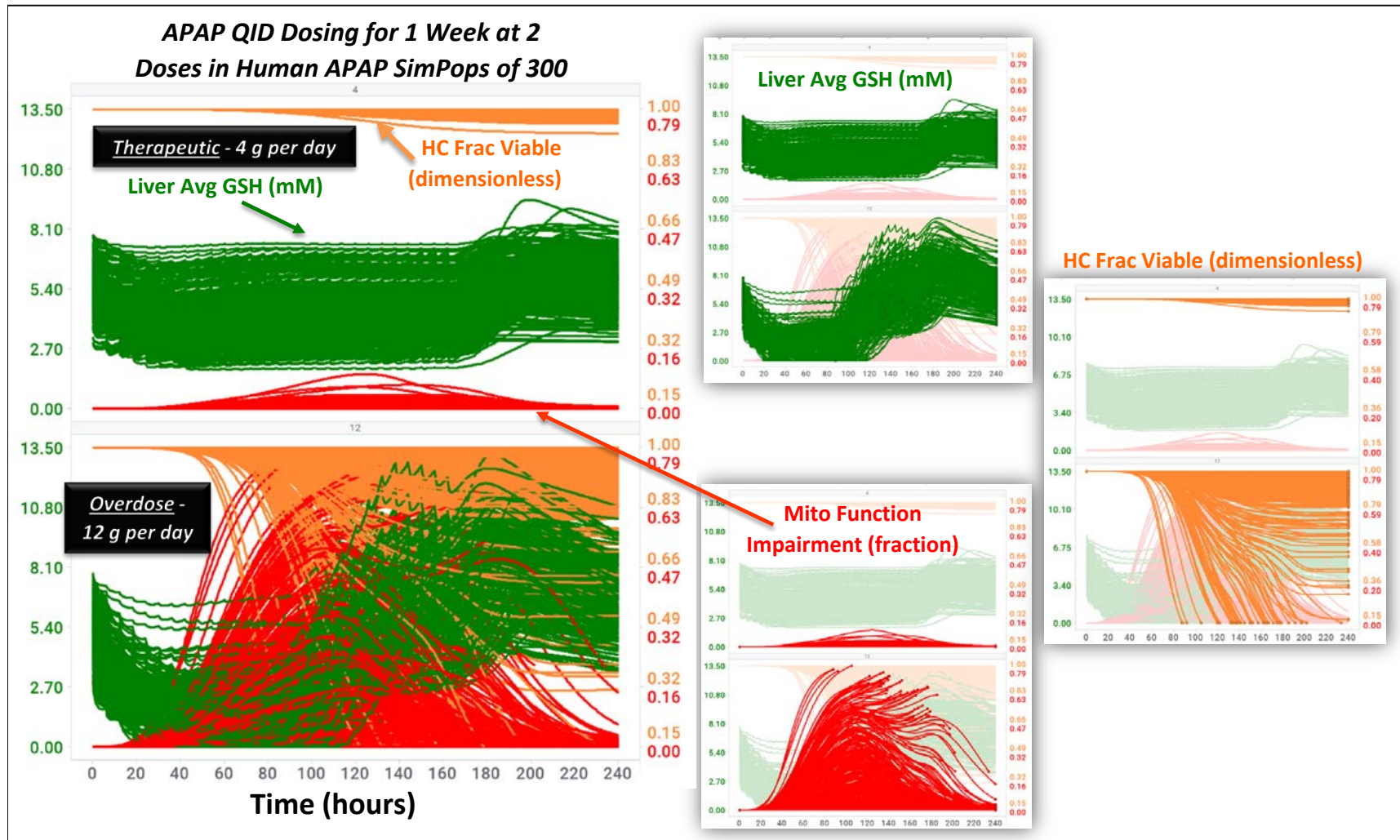
In addition, Figure 25 shows the full population response as a single dose of acetaminophen is escalated. The GSH buffer covers the clinical use case window, while mitochondrial impairment, protein adduction, and cell death all occur as patients get to significantly depleted GSH levels in their livers.

Figure 25: Normalized Range from SimPops of GSH, Mitochondrial Impairment, NAPQI-Protein Adduction, and Cell Death for a Single Dose of acetaminophen Across a Range of Doses
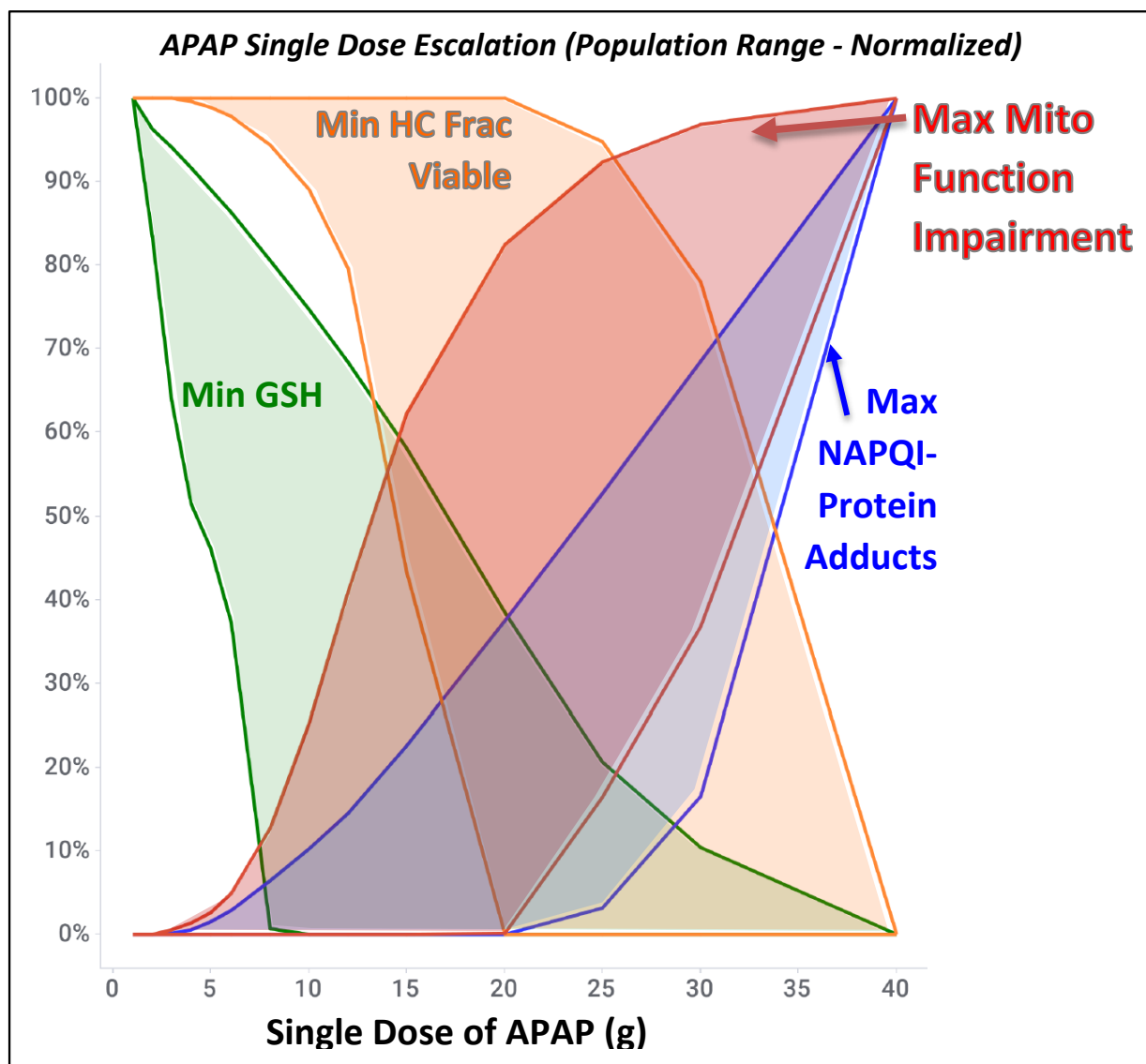
Experimental support for the population level dose response shown in Figure 25 can be found in Davis 1976 (89), as shown below. The study showed that minimal damage to the liver occurred below 10 g of acetaminophen, which is approximately where complete GSH depletion occurs for the most sensitive subject in the simulations. The study also supports the notion that moderate cell death occurs between 10 and 20 g of acetaminophen (range of 0% cell loss to severe cell loss in Figure 25), with the injury becoming more severe beyond 20 g for most people (most of shaded region in Figure 25 has significant cell loss beyond 20 g of acetaminophen).

Table 2: Davis 1976 (89) Study of Human Overdose Cases Showing a Clear Pattern of Liver Damage Starting at About 10 g of acetaminophen and Becoming More Severe Beyond 20 g

TABLE 4. *Relevant data in 30 cases investigated after paracetamol overdose. Biochemical abnormalities are the maximum ones recorded during the course of the illness*

Case	Ingested dose (mmoles) Gram equivalents in brackets	Total urinary recovery of conjugates (mmoles)	Recovery in first 24 hours (mmoles)	AST (I.U.l^{-1})	Plasma bilirubin (μ moles.l^{-1})	Prothrombin time (seconds prolonged)
Minimal liver damage						
1	99 (15)	12·6	12·6	35	8·5	1
2	165 (25)	31·8	31·8	60	13·7	0
3	99 (15)	23·2	23·2	45	8·5	0
4	99 (15)	38·4	38·4	40	10·2	0
5	165 (25)	5·3	5·3	50	13·7	1
6	83 (12·5)	22·5	22·5	35	13·7	0
7	331 (50)	15·9	15·9	46	12·0	0
8	132 (20)	37·1	37·1	40	10·2	0
9	251 (37·5)	36·4	35·7	38	11·9	2
Mild damage						
10	331 (50)	36·4	36·4	368	23·9	4
11	132 (20)	60·9	56·9	763	22·2	3
12	132 (20)	50·3	47·6	80	13·7	4
13	198 (30)	115·8	106·5	300	8·5	3
14	132 (20)	62·2	58·2	175	20·5	6
15	132 (20)	70·1	65·5	600	20·5	4
16	165 (25)	59·6	56·2	348	17·1	3
17	25 (37·5)	52·9	52·9	360	13·7	3
Moderate damage						
18	198 (30)	75·4	64·2	3000	58·1	16
19	232 (35)	69·5	61·5	1600	54·7	15
20	232 (35)	89·5	80·7	5000	46·1	10
21	232 (35)	92·6	86	2450	63·2	24
22	364 (55)	330·9	297·8	2000	53.0	18
23	198 (30)	109·2	93·8	1000	44·4	12
Liver failure						
24	331 (50)	92·0	87·3	5000	97·4	72
25	331+ (50+)	79·4	76·1	3000	167·5	96
26	331 (50)	96	82·7	2500	222·2	63
27	496+ (75+)	119·1	105·9	3500	102·6	85
28	165 (25)	122·4	107·2	2450	188	40
29	165 (25)	45	43·7	4125	164·1	47
30	662 (100)	172·1	156·2	3800	73·5	31

Taken together, Figure 24 and Figure 25 show that across a wide array of patient backgrounds, clinically relevant exposures of acetaminophen do not lead to meaningful cellular stress that would have any impact on carcinogenicity, and that when cellular stress does occur, the levy is breached and cell death also occurs. Where this window of toxicity occurs will vary by patient, but within each patient being considered, the concept of the built-in defense mechanism for acetaminophen holds true.

6 Simulations of Exposures in the Animal Carcinogenicity Studies Compared to Humans Demonstrate Exposure Coverage

6.1 Methods for Exposure and Toxicity Simulations

DILIsym version v8A Patch 1 was used for all simulations described in this document. Physiologically-based pharmacokinetic (PBPK) modeling and hepatotoxicity parameters for acetaminophen in humans, rats, and mice were previously developed and represented within DILIsym (1–3). SimPops are collections of simulated individuals with parameter variability designed to reflect appropriate biochemical and anthropometric ranges. Parameters are selected based on their known or hypothesized biological importance or based on the systematic identification of parameters that critically affect portions of the modeled biochemistry. For human simulations in this work, a previously constructed human SimPops that include variability and acetaminophen exposure and hepatotoxicity parameters (Human_APAP_ROS_apop_mito_v3B_2, n=300) was employed. To assess the coverage of human acetaminophen exposure in animal carcinogenicity studies, four human acetaminophen dosing protocols were simulated (Table 1);

- Therapeutic
    - PO 3 g/day TID for 7 days
    - PO 4 g/day QID for 7 days
- Supratherapeutic
    - PO 8 g/day QID for 7 days
- Acute overdose
    - A single oral dose of 30 g

For rat and mouse simulations in this work, 15 rats and 15 mice with varying sensitivity to acetaminophen-mediated hepatotoxicity were selected from existing rat and mice SimPops (Rat_ROS_apop_mito_v3B_5 and Mouse_ROS_apop_mito_v3B_4), respectively. Because these rat and mice SimPops did not represent variability in acetaminophen exposure, PK variability was simulated by increasing (High PK) or decreasing (Low PK) acetaminophen dose by 10% in addition to the original dose (Medium PK). As a result, each rat and mouse carcinogenicity protocol was simulated in 45 animals with varying acetaminophen exposure and hepatotoxicity parameters. Simulated carcinogenicity protocols are listed in Table 4and Table 5. Acetaminophen hepatotoxicity parameters for rat and mouse were calibrated using mortality data from reported carcinogenicity studies (90) because initial simulations with default parameters predicted significant hepatotoxicity and overpredicted mortality. This is reasonable, since sensitivity to acetaminophen varies greatly by lab, strain, and dosing route within the literature.

6.2 Analysis of Predicted Acetaminophen Exposure in Carcinogenicity Studies

Simulated pharmacokinetic endpoints for human protocols and rodent carcinogenicity protocols are presented in Table 3 and Table 4, respectively. Specifically, the AUC_{0-24hr} were calculated for acetaminophen, acetaminophen-glucuronide, and acetaminophen-sulfate from simulated plasma concentration-time curves of each chemical entity. AUC, not C_{max}, was selected for comparison of PK exposure in humans vs. animals because AUC is less impacted by different patterns of acetaminophen administration; humans were administered acute oral doses whereas animals had continuous

acetaminophen ingestion via food consumption. Because NAPQI is an unstable reactive metabolite, the total amount of NAPQI formed during 24 hr, not hepatic concentration, was calculated and used for comparison.

Table 3: Simulated pharmacokinetic parameters of acetaminophen at different human dosing scenarios. For comparison, *For comparison measured AUC measured in humans at therapeutic doses 221 ± 54 µg*hr/mL (McNeil 2002 – FDA Briefing Book)

Dosing Scenario	Sex	Daily Dose	Duration of Exposure	Pharmacokinetic Endpoints			
				APAP AUC_{0-24hr} (µg*hr/mL)	APAP-Glucuronide AUC_{0-24hr} (µg*hr/mL)	APAP - Sulfate AUC_{0-24hr} (µg*hr/mL)	NAPQI formation (µmol/kg body weight/24 hr)
Therapeutic	M/F	3 g/day	1 week	152.4 ± 36.0	345.4 ± 83.3	103.1 ± 15.3	39.7 ± 12.7
		4 g/day	1 week	203.0 ± 48.8*	447.0 ± 108.3	124.1 ± 16.6	53.2 ± 17.0
Supratherapeutic	M/F	8 g/day	1 week	468.2 ± 118.3	906.2 ± 217.9	181.7 ± 17.5	121.3 ± 38.3
Acute overdose	M/F	Single dose 30 g	Single dose	3944.5 ± 1051.6	3352.0 ± 808.4	269.7 ± 10.5	840.6 ± 232.9

Simulated hepatotoxicity endpoints for each carcinogenicity protocol in rat and mouse are presented in Table 4 and in Figure 26 and Figure 27. Specifically, the minimum fraction viable hepatocytes, peak ALT (i.e., a biomarker of liver injury), and mortality due to hepatotoxicity were analyzed to assess potential hepatotoxicity for each carcinogenicity protocol.

The exposure analysis and simulations support the following conclusions:

- Acetaminophen dose levels for human therapeutic, supratherapeutic, and overdose scenarios were covered by rodent carcinogenicity studies.
- Acetaminophen exposure in human therapeutic and supratherapeutic doses, but not acute overdose, were covered by rat carcinogenicity studies.
- Acetaminophen and NAPQI exposure in human therapeutic, supratherapeutic, and overdose scenarios were covered by mouse carcinogenicity studies.
- Acetaminophen-induced hepatotoxicity is likely to have been present, although was not always reported, in most of mouse study protocols and one rat study protocol.

Table 5 presents a comparison of acetaminophen dose, simulated AUC_{0-24hr} of plasma acetaminophen, and simulated NAPQI formation in rodent carcinogenicity studies to those in human protocols. The ratios of the highest rodent acetaminophen dose in each study to human maximum therapeutic (4 g/day for 7 days) and supratherapeutic (8 g/day for 7 days) doses was greater than 1. The ratios of the highest rodent acetaminophen dose to human overdose (single dose of 30 g) was greater than 1 for all rodent carcinogenicity studies except for rat NTP study where the ratio was 0.7. These results suggest that acetaminophen dosing levels for the human therapeutic, supratherapeutic, and overdose conditions were covered by these four rodent carcinogenicity studies collectively. The ratios of mice acetaminophen exposure to human acetaminophen exposure were smaller than 1 for all three human dosing protocols.

Simulations predicted varying levels of hepatotoxicity for the mouse carcinogenicity protocol simulated. In the NTP 1993 study, no hepatotoxicity was predicted at the lowest dose (i.e., 600 ppm), whereas up to 6% and 9% of mean hepatocyte loss due to acetaminophen hepatotoxicity were predicted for 3000 ppm and 6000 ppm doses, respectively. The magnitude of plasma ALT elevations was not high (59.5 U/L and 142.2 U/L at 3000 ppm and 6000 ppm, respectively, compared to the baseline value of 40 U/L), indicating gradual hepatotoxicity over long-term acetaminophen ingestion (Figure 26). No mortality was predicted for all the dose levels in the NTP 1993 study, consistent with the study report (90).

Table 4: Simulated pharmacokinetic and hepatotoxicity endpoints of acetaminophen in the NTP rodent carcinogenicity studies.

Study	Species	Sex	Diet Exposure (PPM)	Reported Dose (mg/kg)	Duration of Exposure	Pharmacokinetic Endpoints				Hepatotoxicity Endpoints			Indication of Hepatotoxicity
						APAP AUC$_{0-24hr}$ (µg*hr/mL)	APAP-Glucuronide AUC$_{0-24hr}$ (µg*hr/mL)	APAP -Sulfate AUC$_{0-24hr}$ (µg*hr/mL)	NAPQI formation (µmol/kg body weight/24 hr)	Minimum Fraction Viable Hepatocytes	Peak ALT (U/L)*	Mortality[†]	
NTP 1993	Mouse (B6C3F1)	F	600	110	103 wks	9.7 ± 0.9	154.4 ± 13.4	18.8 ± 1.6	386.1 ± 40.0	1.00 ± 0	40.0 ± 0	0/45	No
			3000	600	103 wks	65.3 ± 6.8	977.5 ± 96.9	94.3 ± 7.1	1977.0 ± 194.4	0.94 ± 0.01	59.5 ± 13.9	0/45	Yes
			6000	1200	103 wks	165.8 ± 20.2	2323.3 ± 258.7	168.6 ± 10.9	3588.5 ± 320.4	0.91 ± 0.01	142.2 ± 73.6	0/45	Yes
NTP 1993	Rat (F344/N)	F	600	35	103 wks	0.13 ± 0.01	1.7 ± 0.2	96.6 ± 8.0	0.1 ± 0.02	1.00 ± 0	21.0 ± 0	0/45	No
			3000	160	103 wks	5.44 ± 2.2	26.2 ± 6.2	423.7 ± 30.9	2.4 ± 0.6	1.00 ± 0	21.0 ± 0	0/45	No
			6000	320	103 wks	146.7 ± 36.3	261.6 ± 52.9	604.6 ± 12.7	29.5 ± 6.8	1.00 ± 0	21.0 ± 0	0/45	No

*Baseline ALT levels in DILIsym are 40 U/L and 21 U/L for mouse and rat, respectively.
†The simulated animal "dies" when it loses > 85% of viable hepatocytes within DILIsym.

Table 5: Comparison of acetaminophen dose, acetaminophen exposure, and NAPQI formation in rodent carcinogenicity studies vs. humans

Study	Species	Sex	Diet Exposure (PPM)	Reported Dose (mg/kg)	Duration of Exposure	Ratio of APAP dose (mg/kg) in rodents to human			Ratio of APAP exposure (AUC_{0-24hr}) in rodents to human			Ratio of NAPQI formation (μmol/kg bw/24 hr) in rodents to humans		
						Max Ther. Dose[*]	Supra-ther. Dose	Over dose	Max Ther. Dose[*]	Supra-ther. Dose	Over dose	Max Ther. Dose[*]	Supra-ther. Dose	Over dose
NTP 1993	Mouse (B6C3F1)	F	600	110	103 wks	1.9	1.0	0.3	0.05	0.02	0.002	7.3	3.2	0.5
			3000	600	103 wks	10.5	5.3	1.4	0.3	0.1	0.02	37.1	16.3	2.4
			6000	1200	103 wks	21.0	10.5	2.8	0.8	0.4	0.04	67.4	29.6	4.3
NTP 1993	Rat (F344/N)	F	600	35	103 wks	0.6	0.3	0.1	0.0007	0.0003	0.00003	0.003	0.001	0.0002
			3000	160	103 wks	2.8	1.4	0.4	0.03	0.01	0.001	0.05	0.02	0.003
			6000	320	103 wks	5.6	2.8	0.7	0.7	0.3	0.04	0.6	0.2	0.04

* Maximum therapeutic dose: 4 g/day TID for 7 days.

Figure 26: Simulated fraction viable hepatocytes (a, c, e) and plasma ALT (b, d, f) at the dose of 600 ppm (a and b), 3000 ppm (c and d), and 6000 ppm (e and f) in the mouse NTP 1993 study. Each line represents each simulated animal.
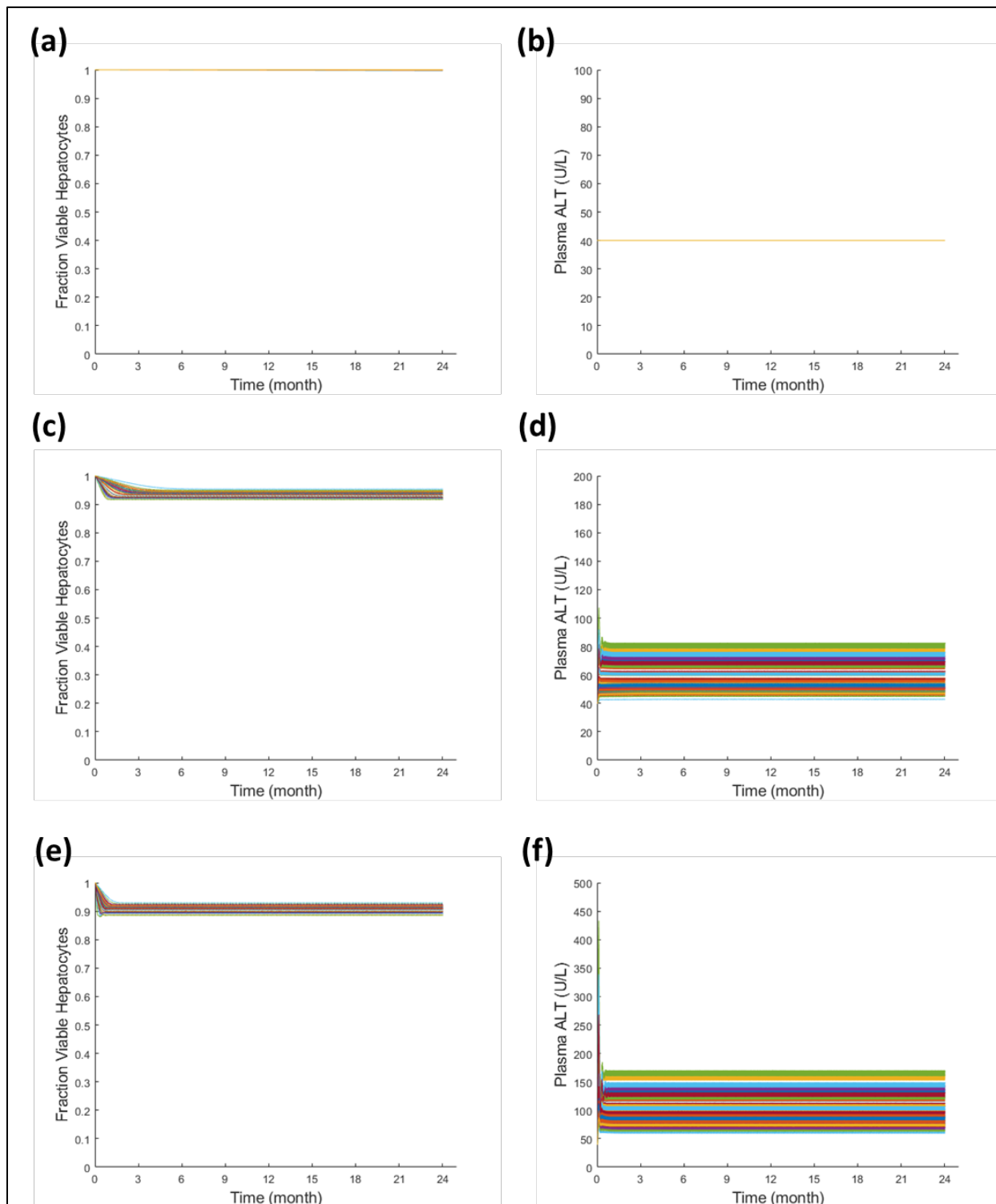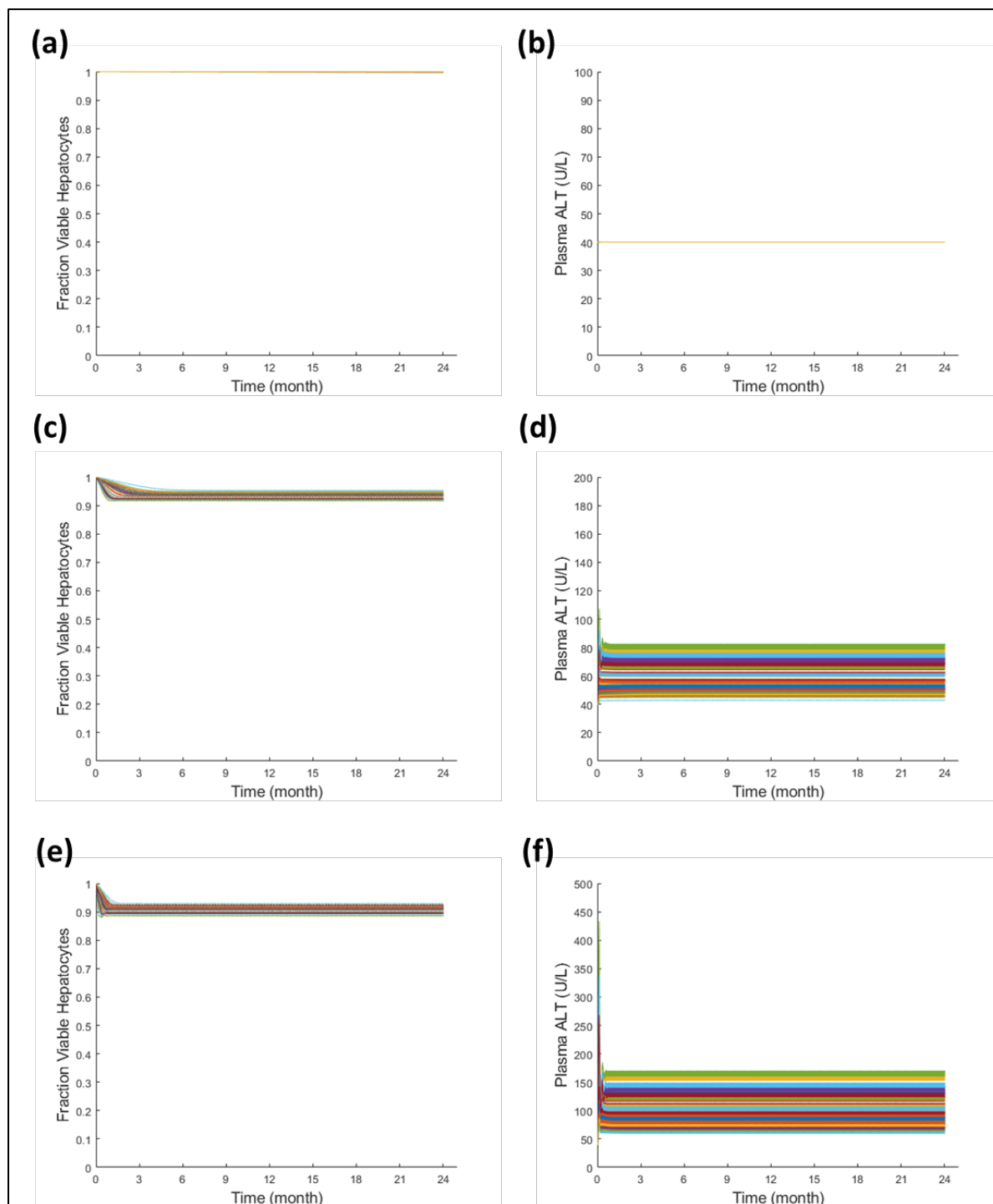
Figure 27: Simulated fraction viable hepatocytes (a, c, e) and plasma ALT (b, d, f) at the dose of 600 ppm (a and b, 3000 ppm (c and d), and 6000 ppm (e and f) in the rat NTP 1993 study. Each line represents each simulated animal.

7   Simulations of Acetaminophen Overdose in Humans Support that Overdose Dose not Result in a Carcinogenicity Hazard

7.1   Overview

Acetaminophen (APAP) overdose simulations were conducted using DILIsym's virtual human population (SimPops) to assess the implications of overdose hepatotoxicity on the likelihood of APAP representing a human hazard for carcinogenicity. Based on the results, the following conclusions can be drawn:

- The overdose SimPops simulations show significant hepatocyte damage that depends on individuals' susceptibility
- For single dose administration of 30 g APAP with N-acetyl cysteine (NAC), most simulated patients recover over time while some do not survive; surviving individuals exhibit significant hepatocyte loss, many showing a loss of 10 - 50% viable hepatocytes;
- Extended SimPops simulations reveal that, over time, surviving patients restore normal liver function through replacement of lost hepatocytes via cellular proliferation and regeneration;
- The SimPops simulation suggest that, under overdose conditions, any potential APAP mediated DNA-damaged cellular domain will encounter hepatocyte loss and then regeneration that ultimately eliminates DNA damaged cells and makes overdose APAP genotoxicity unlikely to occur.

7.2   APAP Overdose SimPops Simulation

To analyze the fate of hepatocytes under APAP overdose conditions and assess any implications for carcinogenicity, we employed the DILIsym APAP model to simulate the toxic effect of a single 30 g dose with N-acetyl cysteine (NAC). NAC is a known antioxidant and glutathione precursor that is often administered to treat patients with APAP overdose. The pharmacokinetics and precursor effects of NAC have been represented and validated in DILIsym using clinical and preclinical data from the literature (3). For APAP overdose simulations, we employed a DILIsym SimPops that represents 300 individuals with pharmacokinetic and hepatotoxic response variability. The overdose simulation was carried out for 7 days and key endpoints were analyzed to provide evidence on the severity of APAP hepatotoxicity and the unlikelihood of APAP carcinogenicity under the acute overdose condition.

7.3   Severe Liver Toxicity Under APAP Overdose Condition

Drug induced liver toxicity is often detected using serum alanine aminotransferase (ALT) and total bilirubin (TBL) as biomarkers. The occurrence of plasma ALT elevations accompanied by increased plasma TBL is the most specific predictor of drug induced hepatotoxicity. Typically, plasma ALT levels that reach three times above the upper limit of normal (ULN) marks meaningful hepatotoxicity. A condition where plasma ALT > 3 X ULN and TBL > 2 X ULN (in DILIsym, the ULN for plasma ALT is 40 U/L and that of total bilirubin is 1 mg/dL) belongs to the notation of a Hy's law case, a situation where the severity of DILI is either fatal or requires liver transplantation in 10% of those cases (91–95). Therefore, the plasma ALT and total bilirubin are used to predict the severity of liver toxicity under APAP overdose conditions.

Figure 28 shows plots of plasma ALT and TBL for the 300 virtual patients at the 30 g dose.

Figure 28: Plasma ALT, plasma TBL and eDISH plot of APAP overdose virtual patients. The eDISH plot depicts the severity and frequency of DILI incidence by dividing the plasma total bilirubin versus plasma ALT plot into four quadrants that represent the normal (ALT < 3 X ULN, TBL < 2 X ULN), hyperbilirubinemia (ALT < 3 X ULN, TBL > 2 X ULN), Temple's corollary (ALT > 3 X ULN, TBL < 2 X ULN), and Hy's law (ALT > 3 X ULN and TBL > 2 X ULN) ranges.
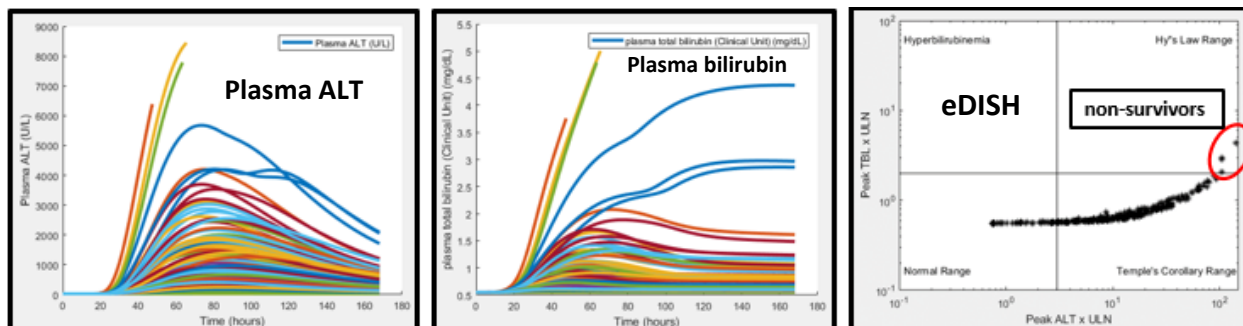

Figure 28 (left) shows significant ALT elevations (much higher than 3 X ULN) under overdose conditions, where the peak in ALT elevations show individual variabilities (a similar behavior is observed for plasma total bilirubin. Most virtual patients exhibit high ALT elevations that resolve to normal over time. On the other hand, extreme cases of overdose exposure are also found in the SimPops simulation where individuals show no recovery. Such behavior is depicted better in the so-called eDISH plot, a graphical representation for the severity and frequency of DILI incidence. The eDISH plot depicted in Figure 28 shows three virtual patients in the Hy's law range, indicating individuals with serious injury. The plot also reveals many virtual patients in the Temple's Corollary (ALT > 3 X ULN, TBL < 2 X ULN) range. Although not as detrimental as the Hy's law case, the high plasma ALT elevations of the Temple's Corollary range signify clinically relevant hepatotoxicity.

Overall, the overdose SimPops simulation reveals significant liver toxicity under overdose conditions.

7.4 Diminished Cellular Viability Under APAP Overdose Conditions

The overdose SimPops simulation shows significant hepatocellular damage depending on the individual's susceptibility. At the cellular level, excessive NAPQI (arising from APAP overdose and GSH depletion) covalently binds with cellular macromolecules and leads to an increase in ROS production. The rise in APAP mediated ROS production is depicted in Figure 29 (Left) where the normalized liver average ROS levels of 300 simulated patients is shown.

Figure 29: Plots of liver average RNS/ROS, liver average GSH and fraction of viable hepatocytes of APAP overdose virtual patients.
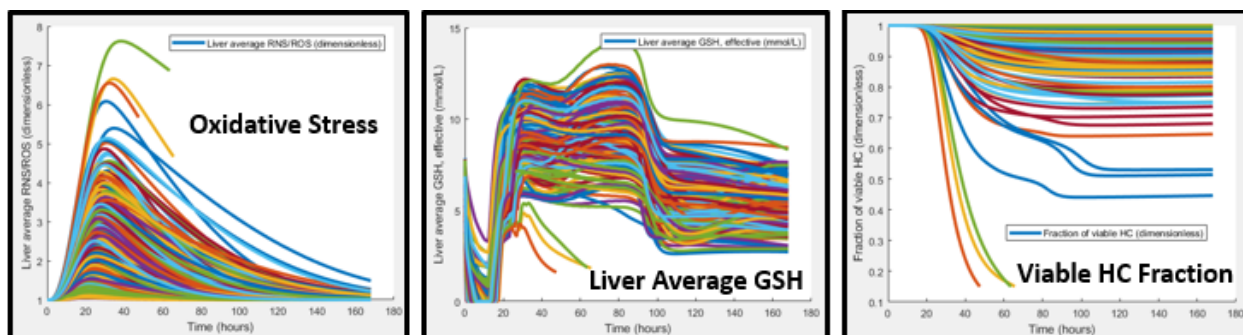
The plot depicts the acute ROS elevations that show individual variation. The variations in individuals' susceptibility against ROS can be partly attributed to the variations in the level of GSH depletion. Figure 29 (middle) demonstrates the variation in the liver average GSH of the virtual human population. The plot shows the early NAPQI mediated decline of liver GSH and delayed recovery through the up-regulation feedback mechanisms including the nuclear factor (erythroid-derived 2)-like 2 response. The plot shows dynamic GSH recovery by all surviving virtual patients, whereas highly susceptible simulated individuals lack such recovery. The combined effect of unregulated ROS elevation and other inter-related intermediate processes (e.g., mitochondrial impairment and ATP decline) results in the onset of hepatocyte loss in the form of necrosis and/or apoptosis. Figure 29 (right) depicts the change in the fraction of viable hepatocytes illustrating APAP mediated hepatocyte loss. The figure reveals that many surviving individuals exhibit significant loss of hepatocytes, some showing up to 50% viable hepatocyte loss. On the other hand, three highly sensitive simulated patients show much higher hepatocyte loss before termination (DILIsym uses 85% loss of viable hepatocyte for termination/death (34,96)), demonstrating fatal cases of acute APAP overdose.

7.5   Immune Response-Mediated Long-Term Cellular Regeneration

To assess long term recovery of APAP overdose patients, we conducted overdose SimPops simulations of a single dose 30 g APAP with NAC for an extended period of time (1 year). The extended SimPops simulations show that, overtime, surviving simulated patients recover through a complex process that involves innate immune responses and hepatocyte proliferation. Briefly, necrotic hepatocytes release damage-associated molecular pattern (DAMP) molecules that stimulate macrophages. Macrophages in turn produce mediators such as TNF and HGF that contribute towards hepatocyte proliferation. Increased proliferation results in the regeneration of hepatocytes that are free of drug toxicity. As an illustration of the intermediate process in this cascade of events, Figure 30 (left) depicts the plot of plasma TNF, a mediator produced due to macrophage stimulation.

Figure 30: Plots of plasma TNF, hepatocyte proliferative flux and fraction of viable hepatocytes for extended simulation of APAP overdose virtual patients
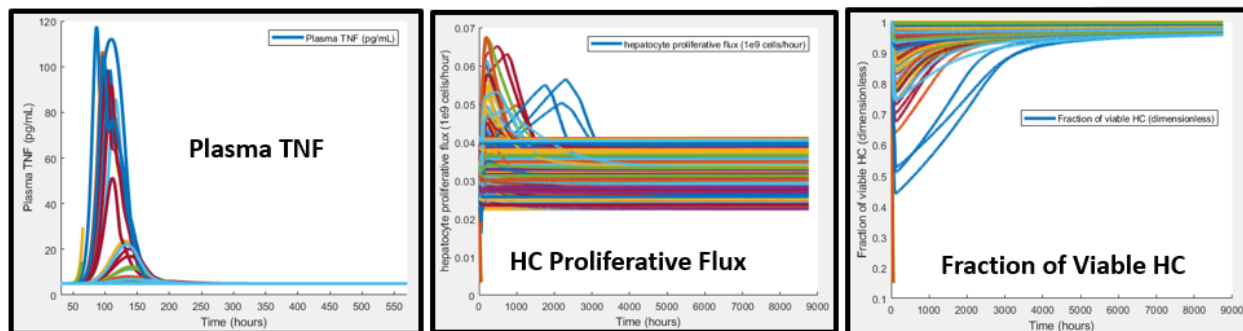

Figure 30 (middle) also shows the amount of hepatocyte proliferation flux for virtual patients that show elevations during the cascade of events leading to recovery. Finally, Figure 30 (right) shows the rise in the fraction of viable hepatocytes as recovery progresses. As shown in the figure, the time for recovery varies among individuals, depending on the injury severity and individual's susceptibility.

Overall, increased hepatocellular proliferation arising from a cascade of events initiated by hepatocyte necrosis allows for the replacement of hepatocytes that are lost due to acute overdose injury, replenishing the liver by renewed hepatocytes that recover normal liver function.

7.6   Implications for Carcinogenicity

Acetaminophen overdose leads to the saturation of sulfation and glucuronidation pathways and GSH depletion, causing increased protein binding with NAPQI and the possibility of DNA binding, although there are no data supporting the latter *in vivo* or in humans. In the liver, under overdose conditions, acetaminophen mediated ROS causes significant hepatocellular injury and death, whereas necrotic hepatocytes stimulate acute immune responses that contribute to hepatocyte proliferation and regeneration. The recycling of hepatocytes under overdose conditions leads to the clearance and replacement of damaged cells that have the potential for carcinogenicity.

Therefore, due to significant hepatocyte loss followed by regeneration of healthy normal liver under overdose conditions, it is unlikely that acetaminophen causes carcinogenicity. Those hepatocytes with damage are more likely to be eliminated by necrosis due to drug toxicity effects and be replaced by renewed hepatocytes.

8   Conclusions

At therapeutic acetaminophen doses across a representative patient population with variations in baseline glutathione, the modeling and simulations results, which are consistent with extensive mechanistic experimental data, support that cellular glutathione deactivates the NAPQI metabolite and there is sufficient buffering capacity to prevent any meaningful protein adduct formation or oxidative stress. As acetaminophen exposures increase after large overdoses, cell death occurs before any adverse conditions occur (e.g. oxidative stress or DNA damage) that could result in carcinogenicity. Simulations on the exposures in the animal carcinogenicity studies and in humans support that the animal carcinogenicity studies adequately evaluated the range of exposure conditions in humans. The modeling and simulation results also support that acetaminophen is not a carcinogenicity hazard to human health under any conditions, including at therapeutic and supratherapeutic doses and an acute overdose.

9 References

1.   Howell BA, Yang Y, Kumar R, Woodhead JL, Harrill AH, Clewell HJ 3rd, et al. In vitro to in vivo extrapolation and species response comparisons for drug-induced liver injury (DILI) using DILIsym™: a mechanistic, mathematical model of DILI. J Pharmacokinet Pharmacodyn. 2012 Oct;39(5):527–41.

2.   Howell BA, Siler SQ, Watkins PB. Use of a systems model of drug-induced liver injury (DILIsym(®)) to elucidate the mechanistic differences between acetaminophen and its less-toxic isomer, AMAP, in mice. Toxicol Lett. 2014 Apr 21;226(2):163–72.

3.   Woodhead JL, Howell BA, Yang Y, Harrill AH, Clewell HJ 3rd, Andersen ME, et al. An analysis of N-acetylcysteine treatment for acetaminophen overdose using a systems model of drug-induced liver injury. J Pharmacol Exp Ther. 2012 Aug;342(2):529–40.

4.   Bhattacharya S, Shoda LKM, Zhang Q, Woods CG, Howell BA, Siler SQ, et al. Modeling drug- and chemical-induced hepatotoxicity with systems biology approaches. Front Physiol. 2012;3:462.

5.   Howell BA, Siler SQ, Shoda LKM, Yang Y, Woodhead JL, Watkins PB. A mechanistic model of drug-induced liver injury AIDS the interpretation of elevated liver transaminase levels in a phase I clinical trial. CPT Pharmacometrics Syst Pharmacol. 2014;3:e98.

6.   Shoda LKM, Woodhead JL, Siler SQ, Watkins PB, Howell BA. Linking physiology to toxicity using DILIsym(®) , a mechanistic mathematical model of drug-induced liver injury. Biopharm Drug Dispos. 2014 Jan;35(1):33–49.

7.   Yang K, Woodhead JL, Watkins PB, Howell BA, Brouwer KL. Systems Pharmacology Modeling Predicts Delayed Presentation and Species Differences in Bile Acid-Mediated Troglitazone Hepatotoxicity. Clin Pharmacol Ther. 2014 Jul 28;589–98.

8.   Woodhead JL, Watkins PB, Howell BA, Siler SQ, Shoda LKM. The role of quantitative systems pharmacology modeling in the prediction and explanation of idiosyncratic drug-induced liver injury. Drug Metab Pharmacokinet. 2017 Feb;32(1):40–5.

9.   Yang Y, Nadanaciva S, Will Y, Woodhead JL, Howell BA, Watkins PB, et al. MITOsym®: A Mechanistic, Mathematical Model of Hepatocellular Respiration and Bioenergetics. Pharm Res. 2014 Dec 12;

10.   Woodhead JL, Yang K, Siler SQ, Watkins PB, Brouwer KLR, Barton HA, et al. Exploring BSEP inhibition-mediated toxicity with a mechanistic model of drug-induced liver injury. Front Pharmacol. 2014;5:240.

11.   Longo DM, Yang Y, Watkins PB, Howell BA, Siler SQ. Elucidating Differences in the Hepatotoxic Potential of Tolcapone and Entacapone With DILIsym(®), a Mechanistic Model of Drug-Induced Liver Injury. CPT Pharmacometrics Syst Pharmacol. 2016 Jan;5(1):31–9.

12.   Yang K, Guo C, Woodhead JL, St Claire RL, Watkins PB, Siler SQ, et al. Sandwich-Cultured Hepatocytes as a Tool to Study Drug Disposition and Drug-Induced Liver Injury. J Pharm Sci. 2016 Feb;105(2):443–59.

13. Woodhead JL, Brock WJ, Roth SE, Shoaf SE, Brouwer KLR, Church R, et al. Application of a Mechanistic Model to Evaluate Putative Mechanisms of Tolvaptan Drug-Induced Liver Injury and Identify Patient Susceptibility Factors. Toxicol Sci. 2017 Jan;155(1):61–74.

14. Shoda LK, Battista C, Siler SQ, Pisetsky DS, Watkins PB, Howell BA. Mechanistic Modelling of Drug-Induced Liver Injury: Investigating the Role of Innate Immune Responses. Gene Regul Syst Bio. 2017;11:1177625017696074.

15. Watkins PB. The DILI-sim Initiative: Insights into Hepatotoxicity Mechanisms and Biomarker Interpretation. Clin Transl Sci. 2019 Mar;12(2):122–9.

16. Woodhead JL, Yang K, Oldach D, MacLauchlin C, Fernandes P, Watkins PB, et al. Analyzing the Mechanisms Behind Macrolide Antibiotic-Induced Liver Injury Using Quantitative Systems Toxicology Modeling. Pharm Res. 2019 Feb 7;36(3):48.

17. Longo DM, Woodhead JL, Walker P, Herédi-Szabó K, Mogyorósi K, Wolenski FS, et al. Quantitative Systems Toxicology Analysis of In Vitro Mechanistic Assays Reveals Importance of Bile Acid Accumulation and Mitochondrial Dysfunction in TAK-875-Induced Liver Injury. Toxicol Sci. 2019 Feb 1;167(2):458–67.

18. Woodhead JL, Paech F, Maurer M, Engelhardt M, Schmitt-Hoffmann AH, Spickermann J, et al. Prediction of Safety Margin and Optimization of Dosing Protocol for a Novel Antibiotic using Quantitative Systems Pharmacology Modeling. Clin Transl Sci. 2018;11(5):498–505.

19. Howell BA, Siler SQ, Barton HA, Joshi EM, Cabal A, Eichenbaum G, et al. Development of quantitative systems pharmacology and toxicology models within consortia: experiences and lessons learned through DILIsym development. Drug Discovery Today: Disease Models. 2016 Dec 1;22:5–13.

20. Shon J, Abernethy DR. Application of systems pharmacology to explore mechanisms of hepatotoxicity. Clin Pharmacol Ther. 2014 Nov;96(5):536–7.

21. Battista C, Yang K, Stahl SH, Mettetal JT, Watkins PB, Siler SQ, et al. Using Quantitative Systems Toxicology to Investigate Observed Species Differences in CKA-Mediated Hepatotoxicity. Toxicol Sci. 2018 Nov 1;166(1):123–30.

22. Generaux G, Lakhani VV, Yang Y, Nadanaciva S, Qiu L, Riccardi K, et al. Quantitative systems toxicology (QST) reproduces species differences in PF-04895162 liver safety due to combined mitochondrial and bile acid toxicity. Pharmacology Research & Perspectives. 2019;7(6):e00523.

23. Yang K, Battista C, Woodhead JL, Stahl SH, Mettetal JT, Watkins PB, et al. Systems pharmacology modeling of drug-induced hyperbilirubinemia: Differentiating hepatotoxicity and inhibition of enzymes/transporters. Clin Pharmacol Ther. 2017 Apr;101(4):501–9.

24. Woodhead JL, Howell BA, Yang Y, Harrill AH, Clewell HJ 3rd, Andersen ME, et al. An analysis of N-acetylcysteine treatment for acetaminophen overdose using a systems model of drug-induced liver injury. J Pharmacol Exp Ther. 2012 Aug;342(2):529–40.

25. Slattery JT, Levy G. Acetaminophen kinetics in acutely poisoned patients. Clin Pharmacol Ther. 1979 Feb;25(2):184–95.

26. Eandi M, Viano I, Ricci Gamalero S. Absolute bioavailability of paracetamol after oral or rectal administration in healthy volunteers. Arzneimittelforschung. 1984;34(8):903–7.

27. Rawlins MD, Henderson DB, Hijab AR. Pharmacokinetics of paracetamol (acetaminophen) after intravenous and oral administration. Eur J Clin Pharmacol. 1977 Apr 20;11(4):283–6.

28. Prescott LF. Kinetics and metabolism of paracetamol and phenacetin. Br J Clin Pharmacol. 1980 Oct;10 Suppl 2:291S-298S.

29. Gelotte CK, Auiler JF, Lynch JM, Temple AR, Slattery JT. Disposition of acetaminophen at 4, 6, and 8 g/day for 3 days in healthy young adults. Clin Pharmacol Ther. 2007 Jun;81(6):840–8.

30. Singer AJ, Carracio TR, Mofenson HC. The temporal profile of increased transaminase levels in patients with acetaminophen-induced liver dysfunction. Ann Emerg Med. 1995 Jul;26(1):49–53.

31. Watkins PB, Seligman PJ, Pears JS, Avigan MI, Senior JR. Using controlled clinical trials to learn more about acute drug-induced liver injury. Hepatology. 2008 Nov;48(5):1680–9.

32. Temple AR, Lynch JM, Vena J, Auiler JF, Gelotte CK. Aminotransferase activities in healthy subjects receiving three-day dosing of 4, 6, or 8 grams per day of acetaminophen. Clin Toxicol (Phila). 2007;45(1):36–44.

33. Dixon RM, Angus PW, Rajagopalan B, Radda GK. 31P magnetic resonance spectroscopy detects a functional abnormality in liver metabolism after acetaminophen poisoning. Hepatology. 1992 Oct;16(4):943–8.

34. Portmann B, Talbot IC, Day DW, Davidson AR, Murray-Lyon IM, Williams R. Histopathological changes in the liver following a paracetamol overdose: correlation with clinical and biochemical parameters. J Pathol. 1975 Nov;117(3):169–81.

35. Aoki T, Imamura H, Matsuyama Y, Kishi Y, Kobayashi T, Sugawara Y, et al. Convergence process of volumetric liver regeneration after living-donor hepatectomy. J Gastrointest Surg. 2011 Sep;15(9):1594–601.

36. Haga J, Shimazu M, Wakabayashi G, Tanabe M, Kawachi S, Fuchimoto Y, et al. Liver regeneration in donors and adult recipients after living donor liver transplantation. Liver Transpl. 2008 Dec;14(12):1718–24.

37. Kwon KH, Kim YW, Kim SI, Kim KS, Lee WJ, Choi JS. Postoperative liver regeneration and complication in live liver donor after partial hepatectomy for living donor liver transplantation. Yonsei Med J. 2003 Dec 30;44(6):1069–77.

38. Nadalin S, Testa G, Malagó M, Beste M, Frilling A, Schroeder T, et al. Volumetric and functional recovery of the liver after right hepatectomy for living donation. Liver Transpl. 2004 Aug;10(8):1024–9.

39. Kwon A-H, Matsui Y, Kaibori M, Kamiyama Y. Functional hepatic regeneration following hepatectomy using galactosyl-human serum albumin liver scintigraphy. Transplant Proc. 2004 Oct;36(8):2257–60.

40. Galinsky RE, Levy G. Dose- and time-dependent elimination of acetaminophen in rats: pharmacokinetic implications of cosubstrate depletion. J Pharmacol Exp Ther. 1981 Oct;219(1):14–20.

41. Hjelle JJ, Klaassen CD. Glucuronidation and biliary excretion of acetaminophen in rats. J Pharmacol Exp Ther. 1984 Feb;228(2):407–13.

42. Saito C, Lemasters JJ, Jaeschke H. c-Jun N-terminal kinase modulates oxidant stress and peroxynitrite formation independent of inducible nitric oxide synthase in acetaminophen hepatotoxicity. Toxicol Appl Pharmacol. 2010 Jul;246(1–2):8–17.

43. Saito C, Yan H-M, Artigues A, Villar MT, Farhood A, Jaeschke H. Mechanism of protection by metallothionein against acetaminophen hepatotoxicity. Toxicol Appl Pharmacol. 2010 Jan 15;242(2):182–90.

44. Saito C, Zwingmann C, Jaeschke H. Novel mechanisms of protection against acetaminophen hepatotoxicity in mice by glutathione and N-acetylcysteine. Hepatology. 2010 Jan;51(1):246–54.

45. James LP, McCullough SS, Lamps LW, Hinson JA. Effect of N-acetylcysteine on acetaminophen toxicity in mice: relationship to reactive nitrogen and cytokine formation. Toxicol Sci. 2003 Oct;75(2):458–67.

46. Vaquero J, Bélanger M, James L, Herrero R, Desjardins P, Côté J, et al. Mild hypothermia attenuates liver injury and improves survival in mice with acetaminophen toxicity. Gastroenterology. 2007 Jan;132(1):372–83.

47. Liu J, Liu Y, Hartley D, Klaassen CD, Shehin-Johnson SE, Lucas A, et al. Metallothionein-I/II knockout mice are sensitive to acetaminophen-induced hepatotoxicity. J Pharmacol Exp Ther. 1999 Apr;289(1):580–6.

48. Muldrew KL, James LP, Coop L, McCullough SS, Hendrickson HP, Hinson JA, et al. Determination of acetaminophen-protein adducts in mouse liver and serum and human serum after hepatotoxic doses of acetaminophen using high-performance liquid chromatography with electrochemical detection. Drug Metab Dispos. 2002 Apr;30(4):446–51.

49. Zhang J-Z, Liu Z, Liu J, Ren J-X, Sun T-S. Mitochondrial DNA induces inflammation and increases TLR9/NF-κB expression in lung tissue. International Journal of Molecular Medicine [Internet]. 2014 Feb 10 [cited 2017 Jul 3]; Available from: http://www.spandidos-publications.com/10.3892/ijmm.2014.1650

50. Lauterburg BH, Corcoran GB, Mitchell JR. Mechanism of action of N-acetylcysteine in the protection against the hepatotoxicity of acetaminophen in rats in vivo. J Clin Invest. 1983 Apr;71(4):980–91.

51. Speeg KV, Mitchell MC, Maldonado AL. Additive protection of cimetidine and N-acetylcysteine treatment against acetaminophen-induced hepatic necrosis in the rat. J Pharmacol Exp Ther. 1985 Sep;234(3):550–4.

52. Jaeschke H. Glutathione disulfide formation and oxidant stress during acetaminophen-induced hepatotoxicity in mice in vivo: the protective effect of allopurinol. J Pharmacol Exp Ther. 1990 Dec;255(3):935–41.

53. Napirei M, Basnakian AG, Apostolov EO, Mannherz HG. Deoxyribonuclease 1 aggravates acetaminophen-induced liver necrosis in male CD-1 mice. Hepatology. 2006 Feb;43(2):297–305.

54. Antoine DJ, Williams DP, Kipar A, Laverty H, Park BK. Diet restriction inhibits apoptosis and HMGB1 oxidation and promotes inflammatory cell recruitment during acetaminophen hepatotoxicity. Mol Med. 2010 Dec;16(11–12):479–90.

55. Hanawa N, Shinohara M, Saberi B, Gaarde WA, Han D, Kaplowitz N. Role of JNK translocation to mitochondria leading to inhibition of mitochondria bioenergetics in acetaminophen-induced liver injury. J Biol Chem. 2008 May 16;283(20):13565–77.

56. Banerjee A, Linscheer WG, Chiji H, Murthy UK, Cho C, Nandi J, et al. Induction of an ATPase inhibitor protein by propylthiouracil and protection against paracetamol (acetaminophen) hepatotoxicity in the rat. Br J Pharmacol. 1998 Jul;124(6):1041–7.

57. Martin FL, McLean AE. Adenosine triphosphate (ATP) levels in paracetamol-induced cell injury in the rat in vivo and in vitro. Toxicology. 1995 Dec 15;104(1–3):91–7.

58. Heinloth AN, Irwin RD, Boorman GA, Nettesheim P, Fannin RD, Sieber SO, et al. Gene expression profiling of rat livers reveals indicators of potential adverse effects. Toxicol Sci. 2004 Jul;80(1):193–202.

59. Maezono K, Kajiwara K, Mawatari K, Shinkai A, Torii K, Maki T. Alanine protects liver from injury caused by F-galactosamine and CCl4. Hepatology. 1996 Jul;24(1):185–91.

60. Aleksunes LM, Slitt AM, Cherrington NJ, Thibodeau MS, Klaassen CD, Manautou JE. Differential expression of mouse hepatic transporter genes in response to acetaminophen and carbon tetrachloride. Toxicol Sci. 2005 Jan;83(1):44–52.

61. Aleksunes LM, Campion SN, Goedken MJ, Manautou JE. Acquired resistance to acetaminophen hepatotoxicity is associated with induction of multidrug resistance-associated protein 4 (Mrp4) in proliferating hepatocytes. Toxicol Sci. 2008 Aug;104(2):261–73.

62. Fujimoto K, Kumagai K, Ito K, Arakawa S, Ando Y, Oda S, et al. Sensitivity of liver injury in heterozygous Sod2 knockout mice treated with troglitazone or acetaminophen. Toxicol Pathol. 2009;37(2):193–200.

63. Campion SN, Johnson R, Aleksunes LM, Goedken MJ, van Rooijen N, Scheffer GL, et al. Hepatic Mrp4 induction following acetaminophen exposure is dependent on Kupffer cell function. Am J Physiol Gastrointest Liver Physiol. 2008 Aug;295(2):G294-304.

64. Henderson NC, Pollock KJ, Frew J, Mackinnon AC, Flavell RA, Davis RJ, et al. Critical role of c-jun (NH2) terminal kinase in paracetamol- induced acute liver failure. Gut. 2007 Jul;56(7):982–90.

65. Bourdi M, Masubuchi Y, Reilly TP, Amouzadeh HR, Martin JL, George JW, et al. Protection against acetaminophen-induced liver injury and lethality by interleukin 10: role of inducible nitric oxide synthase. Hepatology. 2002 Feb;35(2):289–98.

66. Dambach DM, Durham SK, Laskin JD, Laskin DL. Distinct roles of NF-kappaB p50 in the regulation of acetaminophen-induced inflammatory mediator production and hepatotoxicity. Toxicol Appl Pharmacol. 2006 Mar 1;211(2):157–65.

67. Gunawan BK, Liu Z-X, Han D, Hanawa N, Gaarde WA, Kaplowitz N. c-Jun N-terminal kinase plays a major role in murine acetaminophen hepatotoxicity. Gastroenterology. 2006 Jul;131(1):165–78.

68. Nakagawa H, Maeda S, Hikiba Y, Ohmae T, Shibata W, Yanai A, et al. Deletion of apoptosis signal-regulating kinase 1 attenuates acetaminophen-induced liver injury by inhibiting c-Jun N-terminal kinase activation. Gastroenterology. 2008 Oct;135(4):1311–21.

69. Shinohara M, Ybanez MD, Win S, Than TA, Jain S, Gaarde WA, et al. Silencing glycogen synthase kinase-3beta inhibits acetaminophen hepatotoxicity and attenuates JNK activation and loss of glutamate cysteine ligase and myeloid cell leukemia sequence 1. J Biol Chem. 2010 Mar 12;285(11):8244–55.

70. Srinivasan C, Williams WM, Ray MB, Chen TS. Prevention of acetaminophen-induced liver toxicity by 2(R,S)-n-propylthiazolidine-4(R)-carboxylic acid in mice. Biochem Pharmacol. 2001 Jan 15;61(2):245–52.

71. Liu Z-X, Govindarajan S, Kaplowitz N. Innate immune system plays a critical role in determining the progression and severity of acetaminophen hepatotoxicity. Gastroenterology. 2004 Dec;127(6):1760–74.

72. Liu Z-X, Kaplowitz N. Role of innate immunity in acetaminophen-induced hepatotoxicity. Expert Opin Drug Metab Toxicol. 2006 Aug;2(4):493–503.

73. Maddox JF, Amuzie CJ, Li M, Newport SW, Sparkenbaugh E, Cuff CF, et al. Bacterial- and viral-induced inflammation increases sensitivity to acetaminophen hepatotoxicity. J Toxicol Environ Health Part A. 2010;73(1):58–73.

74. Michael SL, Mayeux PR, Bucci TJ, Warbritton AR, Irwin LK, Pumford NR, et al. Acetaminophen-induced hepatotoxicity in mice lacking inducible nitric oxide synthase activity. Nitric Oxide. 2001;5(5):432–41.

75. Yuan H-D, Jin G-Z, Piao G-C. Hepatoprotective effects of an active part from Artemisia sacrorum Ledeb. against acetaminophen-induced toxicity in mice. Journal of ethnopharmacology. 2010 Feb;127(2):528–33.

76. Kojo K, Ito Y, Eshima K, Nishizawa N, Ohkubo H, Yokomizo T, et al. BLT1 signalling protects the liver against acetaminophen hepatotoxicity by preventing excessive accumulation of hepatic neutrophils. Sci Rep [Internet]. 2016 Jul 11 [cited 2019 Oct 22];6. Available from: https://www.ncbi.nlm.nih.gov/pmc/articles/PMC4939602/

77. Gueguen Y, Grandcolas L, Baudelin C, Grison S, Tissandie E, Jourdain J, et al. Effect of acetaminophen administration to rats chronically exposed to depleted uranium. Toxicology. 2007;229(1):62–72.

78. Chen Y-H, Lin F-Y, Liu P-L, Huang Y-T, Chiu J-H, Chang Y-C, et al. Antioxidative and hepatoprotective effects of magnolol on acetaminophen-induced liver damage in rats. Arch Pharm Res. 2009 Feb;32(2):221–8.

79. Sugimura Y, Yamamoto K. Effect of orally administered reduced- and oxidized-glutathione against acetaminophen-induced liver injury in rats. J Nutr Sci Vitaminol. 1998 Oct;44(5):613–24.

80. Wang PY, Kaneko T, Wang Y, Sato A. Acarbose alone or in combination with ethanol potentiates the hepatotoxicity of carbon tetrachloride and acetaminophen in rats. Hepatology. 1999 Jan;29(1):161–5.

81. Waters E, Wang JH, Redmond HP, Wu QD, Kay E, Bouchier-Hayes D. Role of taurine in preventing acetaminophen-induced hepatic injury in the rat. Am J Physiol Gastrointest Liver Physiol. 2001 Jun;280(6):G1274-1279.

82. Zieve L, Anderson WR, Dozeman R, Draves K, Lyftogt C. Acetaminophen liver injury: sequential changes in two biochemical indices of regeneration and their relationship to histologic alterations. J Lab Clin Med. 1985 May;105(5):619–24.

83. Chanda S, Mangipudy RS, Warbritton A, Bucci TJ, Mehendale HM. Stimulated hepatic tissue repair underlies heteroprotection by thioacetamide against acetaminophen-induced lethality. Hepatology. 1995 Feb;21(2):477–86.

84. Ramachandran A, McGill MR, Xie Y, Ni H-M, Ding W-X, Jaeschke H. Receptor interacting protein kinase 3 is a critical early mediator of acetaminophen-induced hepatocyte necrosis in mice. Hepatology. 2013;58(6):2099–2108.

85. Palani S, Raja S, Senthil Kumar B. Hepatoprotective and antioxidant potential of Chloroxylon swietenia (Rutaceae) On Acetaminophen Induced toxicity in Male Albino Rats. International Journal of PharmTech Research. 2010 Mar;2(1):162–70.

86. Gul H, Uysal B, Cakir E, Yaman H, Macit E, Yildirim AO, et al. The protective effects of ozone therapy in a rat model of acetaminophen-induced liver injury. Environ Toxicol Pharmacol. 2012 Jul;34(1):81–6.

87. Kamanaka Y, Kawabata A, Matsuya H, Taga C, Sekiguchi F, Kawao N. Effect of a potent iNOS inhibitor (ONO-1714) on acetaminophen-induced hepatotoxicity in the rat. Life Sci. 2003 Dec 26;74(6):793–802.

88. Potter WZ, Thorgeirsson SS, Jollow DJ, Mitchell JR. Acetaminophen-induced hepatic necrosis. V. Correlation of hepatic necrosis, covalent binding and glutathione depletion in hamsters. Pharmacology. 1974;12(3):129–43.

89. Davis M, Simmons CJ, Harrison NG, Williams R. Paracetamol overdose in man: relationship between pattern of urinary metabolites and severity of liver damage. Q J Med. 1976 Apr;45(178):181–91.

90. National Toxicology Program. NTP Toxicology and Carcinogenesis Studies of Acetaminophen (CAS No. 103-90-2) in F344 Rats and B6C3F1 Mice (Feed Studies). Natl Toxicol Program Tech Rep Ser. 1993 Jan;394:1–274.

91. Senior JR. How can "Hy's law" help the clinician? Pharmacoepidemiol Drug Saf. 2006 Apr;15(4):235–9.

92. Senior JR. Drug hepatotoxicity from a regulatory perspective. Clinics in liver disease. 2007 Aug;11(3):507–24, vi.

93. Senior JR. Alanine aminotransferase: a clinical and regulatory tool for detecting liver injury-past, present, and future. Clinical pharmacology and therapeutics. 2012 Sep;92(3):332–9.

94. Senior JR. Monitoring for hepatotoxicity: what is the predictive value of liver "function" tests? Clin Pharmacol Ther. 2009 Mar;85(3):331–4.

95. Senior JR. What is idiosyncratic hepatotoxicity? What is it not? Hepatology. 2008 Jun;47(6):1813–5.

96. Gazzard BG, Portmann B, Murray-Lyon IM, Williams R. Causes of death in fulminant hepatic failure and relationship to quantitative histological assessment of parenchymal damage. Q J Med. 1975 Oct;44(176):615–26.